

# Second Order Corrector in the Homogenization of a Conductive-Radiative Heat Transfer Problem \*

Grégoire Allaire<sup>†</sup> and Zakaria Habibi<sup>‡</sup>

## Abstract

This paper focuses on the contribution of the so-called second order corrector in periodic homogenization applied to a conductive-radiative heat transfer problem. More precisely, heat is diffusing in a periodically perforated domain with a non-local boundary condition modelling the radiative transfer in each hole. If the source term is a periodically oscillating function (which is the case in our application to nuclear reactor physics), a strong gradient of the temperature takes place in each periodicity cell, corresponding to a large heat flux between the sources and the perforations. This effect cannot be taken into account by the homogenized model, neither by the first order corrector. We show that this local gradient effect can be reproduced if the second order corrector is added to the reconstructed solution.

**Key words :** periodic homogenization, correctors, heat transfer, radiative transfer.

## 1 Introduction

We study heat transfer in a very heterogeneous periodic porous medium. Since the ratio of the heterogeneities period with the characteristic length-scale of the domain, denoted by  $\epsilon$ , is very small in practice, a direct numerical simulation of this phenomenon is either out of reach or very time consuming on any computer. Therefore, the original heterogeneous problem should be replaced by an homogeneous averaged (or effective, or homogenized) one. This approximation can be further improved if one add to the homogenized solution so-called corrector terms which take into account local fluctuations in each periodicity cell. The goal of homogenization theory [6], [7], [15], [25], [27], [36], [37] is to provide a systematic way of finding such effective problems, of reconstructing an accurate

---

\*This work has been supported by the French Atomic Energy and Alternative Energy Commission, DEN/DM2S at CEA Saclay.

<sup>†</sup>CMAF, Ecole Polytechnique, 91128 Palaiseau, & DM2S, CEA Saclay, 91191 Gif sur Yvette, gregoire.allaire@polytechnique.fr

<sup>‡</sup>DM2S/SFME/LTMF, CEA Saclay, 91191 Gif sur Yvette, & CMAF, Ecole Polytechnique, 91128 Palaiseau, zakaria.habibi@polytechnique.edu

solution by introducing these correctors and of rigorously justifying such an approximation by establishing convergence theorems and error estimates. The purpose of this paper is to carry on this program for a model of conductive-radiative heat transfer in a domain periodically perforated by many infinitely small holes and, more specifically, to show that the second order corrector is crucial to achieve a good approximation in the present context.

Although our model could be applied to a large variety of physical problems, our work is motivated by the study of gas-cooled nuclear reactors which are one of the possible concepts for the 4th generation of reactors, considered in the nuclear industry (see [16]). The core of these reactors is composed by many prismatic blocks of graphite in which are inserted the fuel compacts (playing the role of thermal sources). Each block is also periodically perforated by several channels where the coolant (Helium) flows. For simplicity, we consider a cross section (orthogonal to the cylindrical channels) of such a periodic domain (we refer to our other paper [4] for a discussion of the fully 3D case). In a cross section the gas channels are just a periodic distribution of disconnected circular holes (see Figure 1). The total number of holes is very large (of the order of  $10^4$ ) and their size is very small compared to the size of the core. Consequently, the direct numerical analysis of such a model requires a very fine mesh of the periodic domain. This induces a very expensive numerical resolution that becomes impossible for a real geometry of a reactor core. Therefore, our objective is to define a homogenized model, possibly corrected by several cell problems, in order to obtain an approximate solution, which should be less expensive in term of CPU time and memory, and should converge to the exact solution as  $\epsilon$  goes to zero.

The homogenization of the conductive-radiative heat transfer model (8) was already carried out in [3] for the 2D case and in [4] for a generalization to the 3D case. Thus, the originality of the present paper lies in the improvement of the homogenization approximation by taking into account the second order corrector. To be more specific, the improvement is dramatic when there is a large oscillating source term: then a strong temperature gradient appears in each cell between the source support and the holes boundaries where heat flows by exchange with the coolant. These localized gradients do not appear in the homogenized solution (which is expected), neither in the first order corrector (which is more surprising at first sight). Indeed, the first order corrector, defined as a linear combination of the cell solutions (19), can be interpreted as the local fluctuation of the macroscopic temperature. However, it does not take into account the possible microscopic variations of the source term. It is rather the second order corrector which is the first term in the two-scale asymptotic expansion to admit a contribution due to a varying source term. Our numerical results confirm this asymptotic analysis.

The second order corrector is rarely studied in homogenization theory (see nevertheless the textbooks [6], [7], [36], or the paper [17]) and even more seldom used in numerical homogenization algorithms. To our knowledge the only noticeable exception is the early numerical work of Bourgat [8], [9] where a similar phenomenon was emphasized. More precisely, Bourgat showed that the second

order corrector was again the first term in the two-scale asymptotic expansion which is influenced by a strong variation of the diffusion coefficient. Although these two phenomena (oscillating source term and large amplitude of the diffusion tensor) are different, in both cases the conclusion is the same: including the second order corrector in the reconstruction of an approximate solution improves a lot the comparison with the exact solution. One possible reason for the less systematic use of the second order corrector is that, in theory, it brings a correction of order  $\epsilon^2$ , much smaller than some neglected terms of order  $\epsilon$  in the first order correction (including so-called boundary layers). We shall discuss at length this issue below but let us simply claim that, for many simple (or symmetric) geometries like the one considered here, these neglected terms of order  $\epsilon$  turn out to be very small, while the second order term of order  $\epsilon^2$  is much larger since it is proportional to the source term (which is large in our situation). In other words, the improvement is not obtained in the limit when  $\epsilon$  goes to 0, but for fixed values of  $\epsilon$  which, however small, are not negligible in front of other parameters like the magnitude of the source term.

The paper is organized as follows. In Section 2, we define the geometry and the heat transfer model (8). The main properties of the radiative operator are recalled. It is an integral operator, the kernel of which is called the view factor (it amounts to quantify how a point on the hole boundary is illuminated by the other points on this surface). Section 3 is devoted to the formal method of two-scale asymptotic expansions applied to our problem. Its main result is Proposition 3.1 which gives the precise form of the homogenized problem and the so-called cell problems which define the first order corrector of the homogenized solution. Furthermore, Proposition 3.1 furnishes the second order corrector which can be decomposed as a sum of solutions to auxiliary cell problems (see Corollary 3.1). The rigorous mathematical justification of the homogenization process and of the first order approximation (but not of the second order improvement) has already been done in [3] and [4] using the method of two-scale convergence [1], [34]. We shall not reproduce this argument here and we content ourselves in briefly recalling these results in Section 4. Similarly we recall the expected convergence rates in  $\epsilon$  powers of our homogenization method, without any proof. As is well known, the two-scale convergence method does not justify the second order corrector. In truth, such a justification requires, as a preliminary step, to first introduce the  $\epsilon$ -order boundary layers and to characterize the non-oscillating part of the first-order corrector (see (19) and Remark 3.2). This process of constructing boundary layers is, in practice, restricted to rectangular domains and is quite intricate (see e.g. [2], [6], [30], [33]). The determination of the non-oscillating part of the first-order corrector is even more tricky and is rarely done in numerical practice (see [2], [6], [14]). For the sake of brevity we do not reproduce these constructions here and we content ourselves in mentioning them in Section 4. As a matter of fact we shall not attempt to rigorously justify the improvement brought by the second order corrector. We simply claim that, in the geometrical setting under study, the  $\epsilon$ -order boundary layer and the non-oscillating part of the first-order corrector are numerically negligible. Thus, the second order corrector brings a significant qualitative improvement in

the approximation of the true solution, at least from a practical point of view. A formal generalization to the non-linear case is briefly sketched in Section 5. Indeed, the true physical model of radiative transfer is non-linear since the emitted radiations are following the Stefan-Boltzmann law of proportionality to the 4th power of temperature. Taking into account this non-linearity is not difficult for the formal method of two-scale asymptotic expansions. Thus we give the homogenized and cell problems in this case too, all the more since all our numerical computations are performed in this non-linear setting. Eventually Section 6 is devoted to some 2D numerical results for data corresponding to gas-cooled reactors. For this peculiar model the second order corrector is very useful to improve the qualitative behavior of the approximate solution obtained by homogenization. The results of this paper are part of the PhD thesis of the second author [22] and were announced in [21].

## 2 Setting of the problem

The goal of this section is to define the geometry of the periodically perforated domain and to introduce the model of conductive heat transfer problem. For more details we refer to [22] and references therein.

### 2.1 Geometry

Let  $\Omega = \prod_{j=1}^2 (0, L_j)$  be a rectangular open set of  $\mathbb{R}^2$  with positive lengths  $L_j > 0$ . It is periodically divided in  $N(\epsilon)$  small cells  $(Y_{\epsilon,i})_{i=1\dots N(\epsilon)}$ , each of them being equal, up to a translation and rescaling by a factor  $\epsilon$ , to the same unit periodicity cell  $Y = \prod_{j=1}^2 (0, l_j)$  with  $l_j > 0$ . To avoid unnecessary complications with boundary layers (and because this is the case in the physical problem which motivates this study) we assume that the sequence of small positive parameters  $\epsilon$ , going to zero, is such that  $\Omega$  is made up of entire cells only, namely  $L_j/(\epsilon l_j)$  is an integer for any  $j = 1, 2$ .

We define a reference solid cell  $Y^S$  as the cell  $Y$  perforated by a smooth hole occupied by a gas with a known temperature  $T_{gas}$  (see Figures 1 and 2). We denote by  $\Gamma$  the boundary between  $Y^S$  and the hole (which is assumed to be strictly included in  $Y$  so that, upon periodic repetition, a collection of disconnected isolated holes is obtained). Note that, for notational simplicity, we consider only one hole per cell, although there is no difficulty in treating several disjoint holes per cell (as is the case in our numerical tests where there are two holes per cell). Then, we define the domain  $\Omega_\epsilon$  as the union of  $Y_{\epsilon,i}^S$ , where  $Y_{\epsilon,i}^S$  are the translated and rescaled version of  $Y^S$  for  $i = 1, \dots, N(\epsilon)$  (similar to the correspondence between  $Y_{\epsilon,i}$  and  $Y$ ). On the same token we define the entire holes boundary  $\Gamma_\epsilon$  as the union of individual surfaces  $\Gamma_{\epsilon,i}$ . In summary we have

$$\Omega_\epsilon = \bigcup_{i=1}^{N(\epsilon)} Y_{\epsilon,i}^S, \quad \Gamma_\epsilon = \bigcup_{i=1}^{N(\epsilon)} \Gamma_{\epsilon,i}.$$

We define  $x_{0,i}$  as the center of mass of each cell  $Y_{\epsilon,i}$  such that

$$\int_{Y_{\epsilon,i}} (x - x_{0,i}) dx = 0. \quad (1)$$

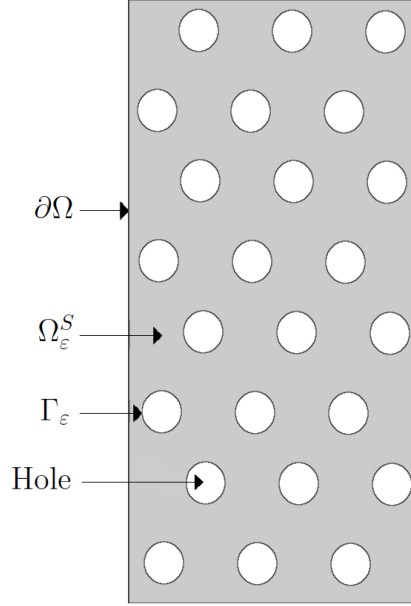


Figure 1: The periodic domain  $\Omega$  (or  $\Omega_\epsilon$ ).

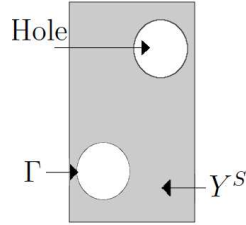


Figure 2: The reference cell  $Y$ .

## 2.2 Governing equations

First, we recall that the current study holds in a simplified 2D setting where convection and diffusion are neglected in the gas. A more complete 3D study, by homogenization, of stationary heat transfer in nuclear reactor cores is undertaken in [4]. In the present 2D setting, heat is transported by conduction in the

solid part  $\Omega_\epsilon$  of the domain and by radiation in the holes  $\Omega \setminus \Omega_\epsilon$ . A non-local boundary condition models the radiative transfer on the hole walls. There is a vast literature on heat transfer and we refer the interested reader to [13], [32], [38] for an introduction to the modelling of radiative transfer.

We denote by  $T_\epsilon$  the temperature in the domain  $\Omega_\epsilon$ . The thermal diffusion tensor in  $\Omega_\epsilon$  is given by

$$K_\epsilon(x) = K(x, \frac{x}{\epsilon}) \quad (2)$$

where  $K(x, y) \in C(\overline{\Omega}; L_\#^\infty(Y))^{2 \times 2}$  is a periodic symmetric positive definite tensor, satisfying

$$\forall v \in \mathbb{R}^2, \forall y \in Y, \forall x \in \Omega, \quad \alpha |v|^2 \leq \sum_{i,j=1}^2 K_{i,j}(x, y) v_i v_j \leq \beta |v|^2,$$

for some constants  $0 < \alpha \leq \beta$ . The gas occupying the holes, being almost transparent, the radiative transfer could be modelled by a non local boundary condition on the boundary  $\Gamma_\epsilon$  between  $\Omega_\epsilon$  and the holes:

$$-K_\epsilon \nabla T_\epsilon \cdot n = \frac{\sigma}{\epsilon} G_\epsilon(T_\epsilon) \quad \text{on } \Gamma_\epsilon, \quad (3)$$

where  $\frac{\sigma}{\epsilon} > 0$  is the Stefan-Boltzmann constant,  $n$  is the unit outward normal on  $\Gamma_\epsilon$  and  $G_\epsilon$  is the radiative operator defined by

$$G_\epsilon(T_\epsilon)(s) = T_\epsilon(s) - \int_{\Gamma_{\epsilon,i}} T_\epsilon(x) F(s, x) dx = (Id - \zeta_\epsilon) T_\epsilon(s) \quad \forall s \in \Gamma_{\epsilon,i}, \quad (4)$$

with

$$\zeta_\epsilon(f)(s) = \int_{\Gamma_{\epsilon,i}} F(s, x) f(x) dx. \quad (5)$$

The scaling  $\epsilon^{-1}$  in front of the radiative operator  $G_\epsilon$  in (3) is chosen because it yields a perfect balance, in the limit as  $\epsilon$  goes to zero, between the bulk heat conduction and the surface radiative transfer (this scaling was first proposed in [3]). In other words, if we perform the change of variables  $y = x/\epsilon$ , then the boundary condition (3) appears at the microscopic scale without any  $\epsilon$  scaling. In (5)  $F$  is the so-called view factor (see [32], [26], [23]) which is a geometrical quantity between two different points  $s$  and  $x$  of the same boundary  $\Gamma_{\epsilon,i}$ . Its explicit formula for surfaces enclosing convex domains in 2D is

$$F(s, x) := \frac{n_x \cdot (s - x) n_s \cdot (x - s)}{2|x - s|^3} \quad (6)$$

where  $n_z$  denotes the unit normal at the point  $z$ .

In truth, some convection and diffusion takes place in the holes due to the gas. It is further modelled by a fixed gas temperature  $T_{gas} \in H^1(\Omega)$  and a heat exchange coefficient, given by

$$h_\epsilon(x) = h(x, \frac{x}{\epsilon})$$

with  $h(x, y) \in C(\overline{\Omega}; L_{\#}^{\infty}(Y))$  satisfying  $h(x, y) \geq 0$ . Then, in absence of radiative transfer, the heat flux on the boundary is

$$-K_{\epsilon} \nabla T_{\epsilon} \cdot n = \epsilon h_{\epsilon}(T_{\epsilon} - T_{gas}) \quad \text{on } \Gamma_{\epsilon}, \quad (7)$$

where the scaling in  $\epsilon$  is such that, again, there is a balance in the homogenized limit between diffusion and exchange with the gas. Actually, we shall use a combination of (3) and (7).

Eventually, the only heat source is a bulk density of thermal sources in the solid part which, furthermore, is an oscillating function given by

$$f_{\epsilon}(x) = f(x, \frac{x}{\epsilon}),$$

with  $f(x, y) \in L^2(\Omega \times Y)$  which is  $Y$ -periodic and satisfies  $f \geq 0$  (see Figure 3 for the geometrical configuration of the support of  $f$ ). The external boundary condition is a simple Dirichlet condition. Thus, the governing equations of our model are

$$\begin{cases} -\operatorname{div}(K_{\epsilon} \nabla T_{\epsilon}) &= f_{\epsilon} & \text{in } \Omega_{\epsilon} \\ -K_{\epsilon} \nabla T_{\epsilon} \cdot n &= \epsilon h_{\epsilon}(T_{\epsilon} - T_{gas}) + \frac{\sigma}{\epsilon} G_{\epsilon}(T_{\epsilon}) & \text{on } \Gamma_{\epsilon} \\ T_{\epsilon} &= 0 & \text{on } \partial\Omega. \end{cases} \quad (8)$$

Applying the Lax-Milgram lemma we easily obtain the following result (see [3] for a proof, if necessary). The main point is that the operator  $G_{\epsilon}$  is self-adjoint and non-negative (see Lemma 2.1).

**Proposition 2.1.** *The boundary value problem (8) admits a unique solution  $T_{\epsilon}$  in  $H^1(\Omega_{\epsilon}) \cap H_0^1(\Omega)$ .*

We recall in Lemma 2.1 some useful properties of the view factor  $F$  and of the radiative operator  $G_{\epsilon}$  (see [22] [29, 38, 39] for further details).

**Lemma 2.1.** *For points  $x$  and  $s$  belonging to the same isolated hole boundary  $\Gamma_{\epsilon, i}$ , the view factor  $F(s, x)$  satisfies*

1.

$$F(s, x) \geq 0, \quad F(s, x) = F(x, s), \quad \int_{\Gamma_{\epsilon, i}} F(s, x) ds = 1, \quad (9)$$

2. *as an operator from  $L^2(\Gamma_{\epsilon, i})$  into itself,*

$$\|\zeta_{\epsilon}\| \leq 1, \quad \text{and} \quad \ker(G_{\epsilon}) = \ker(Id - \zeta_{\epsilon}) = \mathbb{R}, \quad (10)$$

3. *the radiative operator  $G_{\epsilon}$  is self-adjoint on  $L^2(\Gamma_{\epsilon, i})$  and non-negative in the sense that*

$$\int_{\Gamma_{\epsilon, i}} G_{\epsilon}(f) f ds \geq 0 \quad \forall f \in L^2(\Gamma_{\epsilon, i}). \quad (11)$$

The following lemma makes the connection between the radiative operators at the macroscopic and microscopic scales. It will be a key ingredient in the homogenization process.

**Lemma 2.2.** *Define an integral operator  $G$  from  $L^2(\Gamma)$  into  $L^2(\Gamma)$  by*

$$G(\phi)(z) = \phi(z) - \int_{\Gamma} \phi(y) F(z, y) dy. \quad (12)$$

*For any  $\phi \in L^2(\Gamma)$ , introducing  $\phi_{\epsilon}(x) = \phi(\frac{x}{\epsilon})$ , we have*

$$G_{\epsilon}(\phi_{\epsilon})(x) = G(\phi)(\frac{x}{\epsilon}).$$

PROOF This is a simple change of variable  $y = x/\epsilon$  and  $z = s/\epsilon$  using the specific form (6) of the view factor. ■

**Remark 2.1.** *Lemma 2.2 applies to a purely periodic function  $\phi(y)$  but it is no longer true for a locally periodic function  $\phi(x, y)$ . Namely, if  $\phi_{\epsilon}(x) = \phi(x, \frac{x}{\epsilon})$ , then usually*

$$G_{\epsilon}(\phi_{\epsilon})(x) \neq G\left(\phi(x, \cdot)\right)\left(y = \frac{x}{\epsilon}\right).$$

**Remark 2.2.** *The radiation operator introduced in (4) is a linear operator: this is clearly a simplifying assumption. Actually, the true physical radiation operator is non-linear and defined, on each  $\Gamma_{\epsilon, i}$ ,  $1 \leq i \leq N(\epsilon)$ , by*

$$G_{\epsilon}(T_{\epsilon}) = e(Id - \zeta_{\epsilon})(Id - (1 - e)\zeta_{\epsilon})^{-1}(T_{\epsilon}^4). \quad (13)$$

where  $\zeta_{\epsilon}$  is the operator defined by (5). To simplify the exposition, we focus on the case of so-called black walls, i.e., we assume that the emissivity is  $e = 1$  (we can find in [5] a study of this kind of problems when the emissivity depends on the radiation frequency). However, our analysis can be extended straightforwardly to the other cases  $0 < e < 1$  and non-linear operator, at the price of more tedious computations. Therefore we content ourselves in exposing the homogenization process for the linear case. Nevertheless, in Section 5 we indicate how our results can be generalized to the above non-linear setting. Furthermore, our numerical results in Section 6 are obtained in the non-linear case which is more realistic from a physical point of view.

**Remark 2.3.** *As already said in the introduction, the main novelty of the present paper is the introduction of the second order corrector in the approximation of model (8). It is motivated by the appearance of strong gradients of the temperature, solution of (8), between the periodic support of the source term and the holes where heat is exchanged with the exterior. The presence of a radiative term plays no role in this phenomenon which could appear with the mere exchange boundary condition (7). Nevertheless, in a high temperature regime, radiation becomes dominant compared to other means of heat transfer. Therefore, to be physically correct in this study, we take into account the radiative heat transfer.*



### 3 Homogenization

The homogenized problem can be formally obtained by the method of two-scale asymptotic expansion as explained in [6], [7], [15], [36]. It consists in introducing firstly two variables  $x$  and  $y = \frac{x}{\epsilon}$ , where  $x$  is the macroscopic variable and  $y$  is the microscopic one. Secondly, the solution  $T_\epsilon$  of (8) is assumed to be given by the following series

$$T_\epsilon = T_0(x) + \epsilon T_1(x, \frac{x}{\epsilon}) + \epsilon^2 T_2(x, \frac{x}{\epsilon}) + \mathcal{O}(\epsilon^3) \quad (14)$$

where the functions  $y \rightarrow T_i(x, y)$ , for  $i = 1, 2$ , are  $Y$ -periodic. The function  $T_0$  is the homogenized profile of  $T_\epsilon$ , while  $T_1$  is the first order corrector and  $T_2$  the second order corrector. Third, plugging this ansatz in the equations of the model, a cascade of equations are deduced for each term  $T_0, T_1, T_2$ . Finally, the true solution  $T_\epsilon$  can be approximated either by  $T_0$ ,  $(T_0 + \epsilon T_1)$  or  $(T_0 + \epsilon T_1 + \epsilon^2 T_2)$ , depending on our needs for precision.

Introducing (14) in the equations of model (8), we deduce the main result of this section.

**Proposition 3.1.** *Under assumption (14), the zero-order term  $T_0$  of the expansion for the solution  $T_\epsilon$  of (8) is the solution of the homogenized problem*

$$\begin{cases} -\operatorname{div}(K^*(x)\nabla T_0(x)) + h^*(x)(T_0(x) - T_{gas}(x)) = f^*(x) & \text{in } \Omega \\ T_0(x) = 0 & \text{on } \partial\Omega \end{cases} \quad (15)$$

with the homogenized thermal source  $f^*$  and homogenized exchange coefficient  $h^*$  given by simple averages

$$f^*(x) = \frac{1}{|Y|} \int_{Y^S} f(x, y) dy, \quad h^*(x) = \frac{1}{|Y|} \int_{\Gamma} h(x, y) dy, \quad (16)$$

and the homogenized conductivity tensor  $K^*(x)$ , given by its entries, for  $j, k = 1, 2$ ,

$$K_{j,k}^* = \frac{1}{|Y|} \left[ \int_{Y^S} K(e_j + \nabla_y \omega_j) \cdot (e_k + \nabla_y \omega_k) dy + \sigma \int_{\Gamma} G(\omega_k + y_k)(\omega_j + y_j) dy \right], \quad (17)$$

where  $G$  is the microscopic radiative operator defined by (12) and  $(\omega_j(x, y))_{1 \leq j \leq 2}$  are the solutions of the cell problems

$$\begin{cases} -\operatorname{div}_y \left( K(x, y)(e_j + \nabla_y \omega_j) \right) = 0 & \text{in } Y^S \\ -K(x, y)(e_j + \nabla_y \omega_j) \cdot n = \sigma G(\omega_j + y_j) & \text{on } \Gamma \\ y \mapsto \omega_j(y) & \text{is } Y\text{-periodic} \end{cases} \quad (18)$$

Furthermore, the first order corrector  $T_1(x, y)$  can be written

$$T_1(x, y) = \sum_{j=1}^2 \frac{\partial T_0}{\partial x_j}(x) \omega_j(x, y) + \tilde{T}_1(x), \quad (19)$$

and the second order corrector  $T_2(x, y)$  is the solution of the second order cell problem

$$\left\{ \begin{array}{ll} -\operatorname{div}_y \left( K(x, y) [\nabla_y T_2(x, y) + \nabla_x T_1(x, y)] \right) = f(x, y) \\ \quad + \operatorname{div}_x \left( K(x, y) [\nabla_x T_0(x) + \nabla_y T_1(x, y)] \right) & \text{in } Y^S \\ -K(x, y) [\nabla_y T_2(x, y) + \nabla_x T_1(x, y)] \cdot n = h(x, y) \left( T_0(x) - T_{gas}(x) \right) \\ \quad + \sigma G \left( T_2 + \nabla_x T_1 \cdot y + \frac{1}{2} \nabla_x \nabla_x T_0 y \cdot y \right) \\ \quad - \sigma G \left( \nabla_x T_1 + \nabla_x \nabla_x T_0 y \right) \cdot y & \text{on } \Gamma \end{array} \right. \quad (20)$$

$y \mapsto T_2(x, y)$  is  $Y$ -periodic.

**Remark 3.1.** It is proved in [3], [4] that the homogenized tensor  $K^*$ , defined by (17), is symmetric positive definite. Hence, the homogenized equation (15) admits a unique solution  $T_0 \in H_0^1(\Omega)$ .

Furthermore, the following Fredholm alternative is also proved in [3], [4]: for  $p(y) \in L^2_\#(Y^S)$  and  $q(y) \in L^2(\Gamma)$ , there exists a unique solution  $w(y) \in H^1_\#(Y^S)/\mathbb{R}$  (i.e., up to an additive constant) of

$$\left\{ \begin{array}{ll} -\operatorname{div}_y(K \nabla_y w) & = p \quad \text{in } Y^S, \\ -K \nabla_y w \cdot n & = \sigma G(w) - q \quad \text{on } \Gamma, \\ y \mapsto w(y) & \text{is } Y\text{-periodic,} \end{array} \right. \quad (21)$$

if and only if the data satisfy

$$\int_{Y^S} p(y) dy + \int_{\Gamma} q(y) ds(y) = 0. \quad (22)$$

Therefore, it implies that the cell problems (18) admit unique solutions in the same space. Similarly, the second order cell problem (20) admits a unique solution too since the homogenized equation for  $T_0$  is precisely the compatibility condition (22) in the Fredholm alternative.

**Remark 3.2.** The function  $\tilde{T}_1(x)$  appearing in (19) is not specified at this point. It is called the non-oscillating part of the first-order corrector and it will be characterized later in Remark 4.1. The fact that the solution of (21) is merely defined up to an additive constant is the reason for introducing this unknown function  $\tilde{T}_1(x)$  in (19).

**Remark 3.3.** As usual in homogenization, the cell problems (18) and (20) are partial differential equations with respect to the microscopic variable  $y$  while  $x$  plays the role of a parameter. Naively solving cell problems for each value of this parameter  $x$  may increase the cost of the homogenization method. Fortunately, there exist several methods to limit this computational cost. For example, one can use reduced bases methods as in [10], [31], or one can rely on sparse bases on

the tensorial product  $\Omega \times Y$  as in [24]. Nevertheless, if the conductivity tensor depends only on  $y$ , namely  $K(x, y) \equiv K(y)$  (which is the case in our industrial application), the cell problems (18) are completely independent of the parameter  $x$ .

As an immediate corollary of Proposition 3.1, using the linearity of (20) we obtain the following result (see [22] for a proof, if necessary). Note that all second-order cell problems (26), (27) and (28) below are well-posed since they satisfy the compatibility condition (22) of the Fredholm alternative.

**Corollary 3.1.** *Under the same hypotheses than in Proposition 3.1 and assuming further that the conductivity tensor  $K(x, y) \equiv K(y)$  depends only on the microscopic variable and that the functions  $f$  and  $h$  are given by*

$$f(x, y) = F(x)f_{\#}(y) \quad \text{and} \quad h(x, y) = H(x)h_{\#}(y), \quad (23)$$

introducing the averages

$$F^* = \frac{1}{|Y|} \int_{Y^S} f_{\#}(y) dy \quad \text{and} \quad H^* = \frac{1}{|Y|} \int_{\Gamma} h_{\#}(y) dy, \quad (24)$$

the second order corrector  $T_2(x, y)$  can be written

$$\begin{aligned} T_2(x, y) &= T_2^F(y)F(x) + T_2^H(y)H(x)(T_0(x) - T_{gas}(x)) \\ &+ \sum_{i,j=1}^2 \frac{\partial^2 T_0}{\partial x_i \partial x_j}(x) \theta_{i,j}(y) + \tilde{T}_2(x), \end{aligned} \quad (25)$$

where  $T_2^F$ ,  $T_2^H$  and  $\theta_{i,j}$  are the solutions of the second order cell problems

$$\begin{cases} -\operatorname{div}_y \left( K(y) \nabla_y T_2^F(y) \right) &= f_{\#}(y) & \text{in } Y^S \\ -K(y) \nabla_y T_2^F(y) \cdot n &= \frac{|Y|}{|\Gamma|} F^* + \sigma G(T_2^F(y)) & \text{on } \Gamma \\ T_2^F(y) &\text{is } Y\text{-periodic} \end{cases} \quad (26)$$

$$\begin{cases} -\operatorname{div}_y \left( K(y) \nabla_y T_2^H(y) \right) &= 0 & \text{in } Y^S \\ -K(y) \nabla_y T_2^H(y) \cdot n &= (h_{\#}(y) - \frac{|Y|}{|\Gamma|} H^*) + \sigma G(T_2^H(y)) & \text{on } \Gamma \\ T_2^H(y) &\text{is } Y\text{-periodic} \end{cases} \quad (27)$$

and

$$\begin{cases} -\operatorname{div}_y \left( K(y) [\nabla_y \theta_{i,j}(y) + e_j \omega_i(y)] \right) &= K_{i,j}(y) + K(y) \nabla_y \omega_i(y) \cdot e_j & \text{in } Y^S \\ -K(y) [\nabla_y \theta_{i,j}(y) + e_j \omega_i(y)] \cdot n &= \frac{|Y|}{|\Gamma|} K_{i,j}^* \\ &+ \sigma G \left( \theta_{i,j}(y) + \omega_i(y) y_j + \frac{1}{2} y_i y_j \right) - \sigma G \left( \omega_i(y) + y_i \right) y_j & \text{on } \Gamma \\ \theta_{i,j}(y) &\text{is } Y\text{-periodic} \end{cases} \quad (28)$$

**Remark 3.4.** *The first order cell problem (18) does not depend at all on the thermal source  $f$  and on the heat exchange coefficient  $h$ . On the contrary, the cell problem (20) for  $T_2$  does depend on  $f$  and  $h$ . More precisely, Corollary 3.1 shows that the second-order cell problems (26) and (27) depend on the source  $f(x, y)$  and of the coefficient  $h(x, y)$ . Recall that the homogenized problem (15) depends merely on the cell average of  $f$  and  $h$ . Therefore, the interest of the second order corrector  $T_2$  is obvious if one is concerned with the influence of the local variations of  $f$  and  $h$ . As we shall see in the numerical experiments, these microscopic variations are at the root of local temperature gradients for  $T_\epsilon$  which can be reproduced only by  $T_2$ .*

*If there are no local oscillations for the coefficient  $h$ , namely  $h(x, y) \equiv h(x)$ , then the solution of (27) vanishes. Note however that, even if the source term  $f$  is constant, i.e.,  $f(x, y) \equiv f(x)$ , the solution of (26) does not vanish.*

**Remark 3.5.** *The function  $\tilde{T}_2(x)$  appearing in (25) is not specified at this point. It is similar to  $\tilde{T}_1(x)$  in (19) and is due to the non-uniqueness of the solution of (21) as explained in Remark 3.2.*

PROOF (OF PROPOSITION 3.1) As explained in [3, 4], using the method of two scale asymptotic expansions in the strong formulation of problem (8) is cumbersome because of the non-local boundary condition on the holes, arising from the radiative transfer operator. Rather, following an original idea of J.-L. Lions [30], it is simpler to perform this two-scale asymptotic expansion in the weak formulation of (8), thus taking advantage of its symmetry and minimizing the amount of computations. The following proof is essentially an extension of those in [3, 4] (which stopped at first order), going one step further, up to the second order term.

The variational formulation of (8) is: find  $T_\epsilon \in H_0^1(\Omega_\epsilon)$  such that

$$a_\epsilon(T_\epsilon, \phi_\epsilon) = L_\epsilon(\phi_\epsilon) \quad \text{for all function } \phi_\epsilon \in H_0^1(\Omega_\epsilon), \quad (29)$$

with

$$a_\epsilon(T_\epsilon, \phi_\epsilon) = \int_{\Omega_\epsilon} K_\epsilon \nabla T_\epsilon \cdot \nabla \phi_\epsilon dx + \frac{\sigma}{\epsilon} \int_{\Gamma_\epsilon} G(T_\epsilon) \phi_\epsilon dx + \epsilon \int_{\Gamma_\epsilon} h_\epsilon(T_\epsilon - T_{gas}) \phi_\epsilon dx$$

and

$$L_\epsilon(\phi_\epsilon) = \int_{\Omega_\epsilon} f_\epsilon \phi_\epsilon dx.$$

We choose  $\phi_\epsilon$  of the same form than  $T_\epsilon$  in (14), without remainder term,

$$\phi_\epsilon(x) = \phi_0(x) + \epsilon \phi_1(x, \frac{x}{\epsilon}) + \epsilon^2 \phi_2(x, \frac{x}{\epsilon}), \quad (32)$$

with smooth functions  $\phi_0(x)$  and  $\phi_i(x, y)$ ,  $i = 1, 2$ , which are  $Y$ -periodic in  $y$  and have compact support in  $x \in \Omega$ . Inserting the ansatz (14) and (32) in the variational formulation (29) yields

$$\begin{aligned} a^0(T_0, T_1, \phi_0, \phi_1) + \epsilon a^1(T_0, T_1, T_2, \phi_0, \phi_1, \phi_2) &= L^0(\phi_0, \phi_1) + \epsilon L^1(\phi_0, \phi_1, \phi_2) \\ &+ \mathcal{O}(\epsilon^2). \end{aligned} \quad (33)$$

Equating identical powers of  $\epsilon$  we successively obtain:

$$a^0(T_0, T_1, \phi_0, \phi_1) = L^0(\phi_0, \phi_1)$$

which is the two-scale limit variational formulation (in the sense of [1]), namely a combination of the homogenized problem and of the (first order) cell problems, and

$$a^1(T_0, T_1, T_2, \phi_0, \phi_1, \phi_2) = L^1(\phi_0, \phi_1, \phi_2)$$

which yields the second order cell problem defining  $T_2$  (this is the new part compared to [3, 4]).

For the sake of clarity we divide the proof in three steps. The first step is devoted to the ansatz for the diffusion and thermal exchange terms. The second step focuses on the radiation term, while the third one combines these various terms to identify the limit equations. We write the bilinear form in the variational formulation (29) as

$$a_\epsilon(T_\epsilon, \phi_\epsilon) = a_\epsilon^C(T_\epsilon, \phi_\epsilon) + a_\epsilon^R(T_\epsilon, \phi_\epsilon)$$

with

$$\begin{aligned} a_\epsilon^C &= \int_{\Omega_\epsilon} K_\epsilon \nabla T_\epsilon \cdot \nabla \phi_\epsilon dx + \epsilon \int_{\Gamma_\epsilon} h_\epsilon (T_\epsilon - T_{gas}) \phi_\epsilon dx, \\ a_\epsilon^R &= \frac{\sigma}{\epsilon} \int_{\Gamma_\epsilon} G_\epsilon(T_\epsilon) \phi_\epsilon dx. \end{aligned}$$

**Step 1 : Expansion of  $a_\epsilon^C - L_\epsilon$**

This is a standard calculation that we briefly sketch

$$\begin{aligned} a_\epsilon^C - L_\epsilon &= \int_{\Omega_\epsilon} K(\nabla_x T_0 + \nabla_y T_1) \cdot (\nabla_x \phi_0 + \nabla_y \phi_1) dx \\ &+ \epsilon \int_{\Gamma_\epsilon} h(T_0 - T_{gas}) \phi_0 dx \\ &+ \epsilon \int_{\Omega_\epsilon} K(\nabla_x T_1 + \nabla_y T_2) \cdot (\nabla_x \phi_0 + \nabla_y \phi_1) dx \\ &+ \epsilon \int_{\Omega_\epsilon} K(\nabla_x T_0 + \nabla_y T_1) \cdot (\nabla_x \phi_1 + \nabla_y \phi_2) dx \\ &+ \epsilon^2 \int_{\Gamma_\epsilon} h[(T_0 - T_{gas}) \phi_1 + T_1 \phi_0] dx \\ &- \int_{\Omega_\epsilon} f(\phi_0 + \epsilon \phi_1) dx + \mathcal{O}(\epsilon^2) \end{aligned} \tag{34}$$

where all functions are evaluated at  $(x, x/\epsilon)$ . Using Lemma 3.1 below to convert

the integrals on varying domains, we deduce

$$\begin{aligned}
|Y|(a_\epsilon^C - L_\epsilon) = & \\
& \int_{\Omega} \int_{Y^S} K(x, y) (\nabla_x T_0(x) + \nabla_y T_1(x, y) \cdot (\nabla_x \phi_0(x) + \nabla_y \phi_1(x, y))) dy dx \\
& + \int_{\Omega} \int_{\Gamma} h(x, y) (T_0(x) - T_{gas}(x)) \phi_0(x) dy dx - \int_{\Omega} \int_{Y^S} f(x, y) \phi_0(x) dy dx \\
& + \epsilon \left\{ \int_{\Omega} \int_{Y^S} K(x, y) \left[ (\nabla_x T_1(x, y) + \nabla_y T_2(x, y)) \cdot (\nabla_x \phi_0(x) + \nabla_y \phi_1(x, y)) \right. \right. \\
& \quad \left. \left. + (\nabla_x T_0(x) + \nabla_y T_1(x, y)) \cdot (\nabla_x \phi_1(x, y) + \nabla_y \phi_2(x, y)) \right] dy dx \right. \\
& + \int_{\Omega} \int_{\Gamma} h(x, y) \left[ (T_0(x) - T_{gas}(x)) \phi_1(x, y) + T_1(x, y) \phi_0(x) \right] dy dx \\
& \left. - \int_{\Omega} \int_{Y^S} f(x, y) \phi_1(x, y) dy dx \right\} + \mathcal{O}(\epsilon^2).
\end{aligned} \tag{35}$$

**Step 2 : Expansion of  $a_\epsilon^R = a_0^R + \epsilon a_1^R + \mathcal{O}(\epsilon^2)$**

This is the delicate term because the radiative operator  $G_\epsilon$  is integral. Following [3, 4], for both  $T_\epsilon$  and  $\phi_\epsilon$ , we perform a Taylor expansion with respect to the macroscopic variable  $x$  around each center of mass  $x_{0,i}$  of each cell  $Y_{\epsilon,i}$  (the choice of  $x_{0,i}$  or of any other point in the cell  $Y_{\epsilon,i}$  is irrelevant as we shall see in the end). This has the effect that the integral operator  $G_\epsilon$  will apply only to the microscopic variable. Then, according to Lemma 2.2 we can rescale it in the unit cell as  $G$  (in view of Remark 2.1 it is not possible to perform this rescaling if  $G_\epsilon$  applies to functions depending on both  $x$  and  $x/\epsilon$ ). To simplify the notations, we introduce

$$y_{\epsilon,i} = \frac{x - x_{0,i}}{\epsilon}.$$

Then we get

$$\begin{aligned}
T_\epsilon(x) = & T_0(x_{0,i}) + \epsilon \left( \nabla_x T_0(x_{0,i}) \cdot y_{\epsilon,i} + T_1(x_{0,i}, \frac{x}{\epsilon}) \right) \\
& + \epsilon^2 \left( T_2(x_{0,i}, \frac{x}{\epsilon}) + \nabla_x T_1(x_{0,i}, \frac{x}{\epsilon}) \cdot y_{\epsilon,i} + \frac{1}{2} \nabla_x \nabla_x T_0(x_{0,i}) y_{\epsilon,i} \cdot y_{\epsilon,i} \right) \\
& + \epsilon^3 \widehat{T}_{3,\epsilon}(x) + \mathcal{O}(\epsilon^4)
\end{aligned} \tag{36}$$

and

$$\begin{aligned}
\phi_\epsilon(x) = & \phi_0(x_{0,i}) + \epsilon \left( \nabla_x \phi_0(x_{0,i}) \cdot y_{\epsilon,i} + \phi_1(x_{0,i}, \frac{x}{\epsilon}) \right) \\
& + \epsilon^2 \left( \phi_2(x_{0,i}, \frac{x}{\epsilon}) + \nabla_x \phi_1(x_{0,i}, \frac{x}{\epsilon}) \cdot y_{\epsilon,i} + \frac{1}{2} \nabla_x \nabla_x \phi_0(x_{0,i}) y_{\epsilon,i} \cdot y_{\epsilon,i} \right) \\
& + \epsilon^3 \widehat{\phi}_{3,\epsilon}(x) + \mathcal{O}(\epsilon^4)
\end{aligned} \tag{37}$$

where the precise form of the terms  $\widehat{T}_{3,\epsilon}$  and  $\widehat{\phi}_{3,\epsilon}$  is not important since the  $\mathcal{O}(\epsilon^3)$ -order terms will cancel by simplification as we shall soon see.

Recall from Lemma 2.1 that  $G_\epsilon$  is self-adjoint and  $\ker(G_\epsilon) = \mathbb{R}$ . Thus,  $G_\epsilon(T_0(x_{0,i})) = G_\epsilon(\phi_0(x_{0,i})) = 0$  and it yields the following simplified expression

$$\begin{aligned}
& \frac{\sigma}{\epsilon} \int_{\Gamma_{\epsilon,i}} G_\epsilon(T_\epsilon) \phi_\epsilon dx = \\
& \sigma \epsilon \int_{\Gamma_{\epsilon,i}} G_\epsilon \left( \nabla_x T_0(x_{0,i}) \cdot y_{\epsilon,i} + T_1(x_{0,i}, \frac{x}{\epsilon}) \right) \left( \nabla_x \phi_0(x_{0,i}) \cdot y_{\epsilon,i} + \phi_1(x_{0,i}, \frac{x}{\epsilon}) \right) dx \\
& + \sigma \epsilon^2 \int_{\Gamma_{\epsilon,i}} G_\epsilon \left( \nabla_x T_0(x_{0,i}) \cdot y_{\epsilon,i} + T_1(x_{0,i}, \frac{x}{\epsilon}) \right) \left( \phi_2(x_{0,i}, \frac{x}{\epsilon}) \right. \\
& \quad \left. + \nabla_x \phi_1(x_{0,i}, \frac{x}{\epsilon}) \cdot y_{\epsilon,i} + \frac{1}{2} \nabla_x \nabla_x \phi_0(x_{0,i}) y_{\epsilon,i} \cdot y_{\epsilon,i} \right) dx \\
& + \sigma \epsilon^2 \int_{\Gamma_{\epsilon,i}} G_\epsilon \left( \nabla_x \phi_0(x_{0,i}) \cdot y_{\epsilon,i} + \phi_1(x_{0,i}, \frac{x}{\epsilon}) \right) \left( T_2(x_{0,i}, \frac{x}{\epsilon}) \right. \\
& \quad \left. + \nabla_x T_1(x_{0,i}, \frac{x}{\epsilon}) \cdot y_{\epsilon,i} + \frac{1}{2} \nabla_x \nabla_x T_0(x_{0,i}) y_{\epsilon,i} \cdot y_{\epsilon,i} \right) dx \\
& + \mathcal{O}(\epsilon^4),
\end{aligned} \tag{38}$$

where we used  $|\Gamma_{\epsilon,i}| = \epsilon |\Gamma|$  in the remainder term. We can now make the change of variables  $y - y_0 = (x - x_{0,i})/\epsilon$  in (38), with  $y_0$  the center of mass of  $Y$ , and apply Lemma 2.2 to get

$$\begin{aligned}
& \frac{\sigma}{\epsilon} \int_{\Gamma_{\epsilon,i}} G_\epsilon(T_\epsilon) \phi_\epsilon dx = \sigma \epsilon^2 \int_{\Gamma} G \left( \nabla_x T_0(x_{0,i}) \cdot (y - y_0) + T_1(x_{0,i}, y) \right) \left( \phi_1(x_{0,i}, y) \right. \\
& \quad \left. + \nabla_x \phi_0(x_{0,i}) \cdot (y - y_0) \right) dy \\
& + \sigma \epsilon^3 \int_{\Gamma} G \left( \nabla_x T_0(x_{0,i}) \cdot (y - y_0) + T_1(x_{0,i}, y) \right) \left( \phi_2(x_{0,i}, y) \right. \\
& \quad \left. + \nabla_x \phi_1(x_{0,i}, y) \cdot (y - y_0) + \frac{1}{2} \nabla_x \nabla_x \phi_0(x_{0,i}) (y - y_0) \cdot (y - y_0) \right) dy \\
& + \sigma \epsilon^3 \int_{\Gamma} G \left( \nabla_x \phi_0(x_{0,i}) \cdot (y - y_0) + \phi_1(x_{0,i}, y) \right) \left( T_2(x_{0,i}, y) \right. \\
& \quad \left. + \nabla_x T_1(x_{0,i}, y) \cdot (y - y_0) + \frac{1}{2} \nabla_x \nabla_x T_0(x_{0,i}) (y - y_0) \cdot (y - y_0) \right) dy \\
& + \mathcal{O}(\epsilon^4).
\end{aligned} \tag{39}$$

Summing with respect to  $i$  and applying Lemma 3.1 shows that (39) is a Riemann sum approximating an integral over  $\Omega$ , namely

$$a_\epsilon^R = \frac{\sigma}{\epsilon} \sum_{i=1}^{N(\epsilon)} \int_{\Gamma_{\epsilon,i}} G_\epsilon(T_\epsilon) \phi_\epsilon dx = a_0^R + \epsilon a_1^R + \mathcal{O}(\epsilon^2),$$

with

$$a_0^R = \frac{\sigma}{|Y|} \int_{\Omega} \int_{\Gamma} G \left( \nabla_x T_0(x) \cdot (y - y_0) + T_1(x, y) \right) \left( \phi_1(x_{0,i}, y) + \nabla_x \phi_0(x_{0,i}) \cdot (y - y_0) \right) dx dy \quad (40)$$

and

$$\begin{aligned} a_1^R &= \frac{\sigma}{|Y|} \int_{\Omega} \int_{\Gamma} G \left( \nabla_x T_0(x) \cdot (y - y_0) + T_1(x, y) \right) \left( \phi_2(x, y) + \nabla_x \phi_1(x, y) \cdot (y - y_0) + \frac{1}{2} \nabla_x \nabla_x \phi_0(x) (y - y_0) \cdot (y - y_0) \right) dx dy \\ &+ \frac{\sigma}{|Y|} \int_{\Omega} \int_{\Gamma} G \left( \nabla_x \phi_0(x) \cdot (y - y_0) + \phi_1(x, y) \right) \left( T_2(x, y) + \nabla_x T_1(x, y) \cdot (y - y_0) + \frac{1}{2} \nabla_x \nabla_x T_0(x) (y - y_0) \cdot (y - y_0) \right) dx dy. \end{aligned} \quad (41)$$

**Step 3 : Identification of the limit variational formulations**

The zero-th order  $\epsilon^0$ -term of (33), namely  $a^0(T_0, T_1, \phi_0, \phi_1) = L^0(\phi_0, \phi_1)$  is equivalent to

$$\begin{aligned} & \int_{\Omega} \int_{Y^S} K(x, y) (\nabla_x T_0(x) + \nabla_y T_1(x, y) \cdot (\nabla_x \phi_0(x) + \nabla_y \phi_1(x, y))) dx dy \\ & + \int_{\Omega} \int_{\Gamma} h(x, y) (T_0(x) - T_{gas}(x)) \phi_0(x) dx dy \\ & + \sigma \int_{\Omega} \int_{\Gamma} G \left( \nabla_x T_0(x) \cdot (y - y_0) + T_1(x, y) \right) \left( \phi_1(x, y) + \nabla_x \phi_0(x) \cdot (y - y_0) \right) dx dy \\ & = \int_{\Omega} \int_{Y^S} f(x, y) \phi_0(x) dx dy, \end{aligned} \quad (42)$$

which is just the variational formulation of the so-called two-scale limit problem which is a combination of the homogenized and cell problems. Remark that, since  $\ker(G) = \mathbb{R}$ , the terms containing  $y_0$  cancel in (42) which thus does not depend on the choice of reference point  $y_0$ . We recover the cell problem (18) and formula (19) for  $T_1$  by taking  $\phi_0 = 0$  in (42). Then, to recover the homogenized problem (15) we take  $\phi_1 = 0$  in (42). It yields the variational formulation of (15), as well as the formula for  $K^*$ .

The first order  $\epsilon$ -term of (33), namely  $a^1(T_0, T_1, T_2, \phi_0, \phi_1, \phi_2) = L^1(\phi_0, \phi_1, \phi_2)$



is equivalent to

$$\begin{aligned}
& \int_{\Omega} \int_{Y^S} K \left[ (\nabla_x T_1 + \nabla_y T_2) \cdot (\nabla_x \phi_0 + \nabla_y \phi_1) \right. \\
& \quad \left. + (\nabla_x T_0 + \nabla_y T_1) \cdot (\nabla_x \phi_1 + \nabla_y \phi_2) \right] dy dx \\
& + \int_{\Omega} \int_{\Gamma} h \left[ (T_0 - T_{gas}) \phi_1 + T_1 \phi_0 \right] dy dx + a_1^R = \int_{\Omega} \int_{Y^S} f \phi_1 dy dx.
\end{aligned} \tag{43}$$

We recover the second order cell problem (20) for  $T_2$  by choosing  $\phi_0 = 0$  and  $\phi_2 = 0$  in (43)

$$\begin{aligned}
& \int_{\Omega} \int_{Y^S} K \left[ (\nabla_x T_1 + \nabla_y T_2) \cdot \nabla_y \phi_1 + (\nabla_x T_0 + \nabla_y T_1) \cdot \nabla_x \phi_1 \right] dx dy \\
& + \int_{\Omega} \int_{\Gamma} h (T_0 - T_{gas}) \phi_1 dx dy \\
& + \sigma \int_{\Omega} \int_{\Gamma} G \left( \nabla_x T_0 \cdot (y - y_0) + T_1 \right) \nabla_x \phi_1 \cdot (y - y_0) dx dy \\
& + \sigma \int_{\Omega} \int_{\Gamma} \phi_1 G \left( T_2 + \nabla_x T_1 \cdot (y - y_0) + \frac{1}{2} \nabla_x \nabla_x T_0 (y - y_0) \cdot (y - y_0) \right) dx dy \\
& = \int_{\Omega} \int_{Y^S} f(x, y) \phi_1(x, y) dx dy.
\end{aligned} \tag{44}$$

Since  $\phi_1$  belongs to  $H_0^1(\Omega)$ , we can perform an integration by part with respect to  $x$  in the third line of (44) and, using again  $\ker(G) = \mathbb{R}$ , we get

$$\begin{aligned}
& \int_{\Omega} \int_{\Gamma} G \left( \nabla_x T_0 \cdot (y - y_0) + T_1 \right) \nabla_x \phi_1 \cdot (y - y_0) dx dy = \\
& - \int_{\Omega} \int_{\Gamma} G \left( \nabla_x \nabla_x T_0 \cdot y + \nabla_x T_1 \right) \cdot (y - y_0) \phi_1 dx dy.
\end{aligned}$$

Thus, all terms containing  $y_0$  cancel in (44) and we exactly obtain the variational formulation of (20). This finishes the proof of Proposition 3.1.  $\blacksquare$

**Remark 3.6.** In the proof of Proposition 3.1 we obtain the variational formulation (44) for  $T_2$  by making a special choice,  $\phi_0 = 0$  and  $\phi_2 = 0$ , in (43). One may wonder what could be deduced from (43) by another choice. It turns out that choosing  $\phi_2 \neq 0$  yields again the first-order cell problem for  $T_1$ . On the contrary, choosing  $\phi_0 \neq 0$  leads to a new macroscopic equation for the non oscillating first-order corrector  $\tilde{T}_1(x)$  (see Remark 4.1 below).

On the other hand, the proof of Proposition 3.1 cannot possibly detect any boundary layers involved in the asymptotic behavior of  $T_\epsilon$ . The reason is that the test function is assumed to have compact support in  $\Omega$  (a crucial assumption which is used in Lemma 3.1 below). In other words, the results of Proposition 3.1 holds true in the interior of the domain, not on its boundary.

We recall a classical lemma used in the proof of Proposition 3.1.

**Lemma 3.1.** *Let  $g(x, y)$  be a  $Y$ -periodic function in  $L^1_{\#}(Y; C^2(\Omega))$ , with compact support in  $x \in \Omega$ . It satisfies*

$$\begin{aligned} i. \quad & \int_{\Omega_\epsilon} g(x, \frac{x}{\epsilon}) dx = \frac{1}{|Y|} \int_{\Omega} \int_{Y^S} g(x, y) dy dx + \mathcal{O}(\epsilon^2), \\ ii. \quad & \epsilon \int_{\Gamma_\epsilon} g(x, \frac{x}{\epsilon}) dx = \frac{1}{|Y|} \int_{\Omega} \int_{\Gamma} g(x, y) dx dy + \mathcal{O}(\epsilon^2), \\ iii. \quad & \epsilon^2 \sum_{i=1}^{N(\epsilon)} \int_{\Gamma} g(x_{0,i}, y) dy = \frac{1}{|Y|} \int_{\Omega} \int_{\Gamma} g(x, y) dx dy + \mathcal{O}(\epsilon^2). \end{aligned}$$

## 4 Mathematical convergence

The mathematically rigorous justification of that part of Proposition 3.1 concerning the two first terms  $T_0$  and  $\epsilon T_1$  in the expansion (14) has been done in [3] and [4] (with a slightly modified model) using the two scale convergence method [1], [34]. We shall not reproduce this argument and we content ourselves in recalling their main theorem.

**Theorem 4.1 ([3], [4]).** *Let  $T_\epsilon \in H^1(\Omega_\epsilon) \cap H^1_0(\Omega)$  be the sequence of solutions of (8). There exists a positive constant  $C$ , which does not depend on  $\epsilon$ , such that*

$$\|T_\epsilon\|_{H^1(\Omega_\epsilon)} \leq C. \quad (45)$$

Furthermore,  $T_\epsilon$  two-scale converges to  $T_0(x)$  and  $\nabla T_\epsilon$  two-scale converges to  $\nabla_x T_0(x) + \nabla_y T_1(x, y)$ , where  $T_0 \in H^1_0(\Omega)$  is the solution of the homogenized problem (15) and  $T_1(x, y) \in L^2(\Omega; H^1_{\#}(Y^S))$  is the first order corrector defined by (19).

The main novelty of the present work is the second-order corrector  $T_2$  which improves the approximation by homogenization of problem (8) in the presence of an oscillating heat source. Unfortunately, the two-scale convergence method cannot justify it. The usual approach to justify  $T_2$  is to write the equation satisfied by the remainder term

$$r_\epsilon = T_\epsilon - \left( T_0(x) + \epsilon T_1(x, \frac{x}{\epsilon}) + \epsilon^2 T_2(x, \frac{x}{\epsilon}) + \epsilon^3 T_3(x, \frac{x}{\epsilon}) \right) \quad (46)$$

(note the necessary presence of the next order term  $T_3$ ) and to get uniform a priori estimate showing that  $r_\epsilon$  is small in some norm [6], [7]. Solving for  $T_3$  requires a compatibility condition (see the Fredholm alternative in Remark 3.1) which delivers a macroscopic equation for the (so far unknown) non oscillating first-order corrector  $\tilde{T}_1(x)$  appearing in (19) (for more details, see Remark 4.1). However, there is one (serious) additional hurdle in the justification of  $T_2$  which

is that (14) is not a correct ansatz for  $T_\epsilon$  (or equivalently (46) is not accurate) since it is missing boundary layers. The reason is that each corrector,  $T_1$ ,  $T_2$ ,  $T_3$ , does not verify the Dirichlet boundary condition on  $\partial\Omega$ . Because of this, it is impossible to prove that  $r_\epsilon$ , defined by (46), is small. To circumvent this difficulty, boundary layers have to be taken into account. It amounts to replace the former ansatz (14) by the new one

$$T_\epsilon(x) = T_0(x) + \epsilon \left[ T_1(x, \frac{x}{\epsilon}) + T_1^{bl,\epsilon}(x) \right] + \epsilon^2 \left[ T_2(x, \frac{x}{\epsilon}) + T_2^{bl,\epsilon}(x) \right] + \dots, \quad (47)$$

where each function  $T_i^{bl,\epsilon}(x)$ , called a boundary layer, satisfies

$$\begin{cases} -\operatorname{div}(K_\epsilon \nabla T_i^{bl,\epsilon}) &= 0 & \text{in } \Omega, \\ -K_\epsilon \nabla T_i^{bl,\epsilon} \cdot n &= \epsilon h_\epsilon T_i^{bl,\epsilon} + \frac{\sigma}{\epsilon} G_\epsilon(T_i^{bl,\epsilon}) & \text{on } \Gamma_\epsilon, \\ T_i^{bl,\epsilon}(x) &= -T_i(x, \frac{x}{\epsilon}) & \text{on } \partial\Omega. \end{cases} \quad (48)$$

The advantage of the new ansatz (47) is that each term  $T_i + T_i^{bl,\epsilon}$  satisfies a homogeneous Dirichlet boundary condition. On the other hand, it is clear that in (47) the first boundary layer  $T_1^{bl,\epsilon}$  is more important than the second order corrector  $T_2$ .

The asymptotic analysis of (48) is delicate since  $T_i^{bl,\epsilon}(x)$  is not uniformly bounded in the usual energy spaces (the Dirichlet boundary data is not bounded in  $H^{1/2}(\partial\Omega)$ ). It has merely been carried out for rectangular domains having boundaries parallel to the unit cell axes. In such a case, it is proved that  $T_i^{bl,\epsilon}(x)$  is of order 1 in the vicinity of the boundary  $\partial\Omega$  and decays exponentially fast to 0 inside  $\Omega$  (upon a suitable choice of the additive function  $\tilde{T}_i(x)$  in the definition of  $T_i(x, y)$ ); hence its name of boundary layers (see [2], [6], [7], [11], [18], [19], [20], [28], [30], [33], [35] for more details in the case of a pure conduction problem). In general, boundary layers should satisfy the following a priori estimates

$$\|T_i^{bl}\|_{H^1(\Omega)} = \mathcal{O}(\frac{1}{\sqrt{\epsilon}}), \quad \|T_i^{bl}\|_{L^2(\Omega)} = \mathcal{O}(1), \quad \|T_i^{bl}\|_{H^1(\omega)} = \mathcal{O}(1) \quad \text{for all } \omega \subset\subset \Omega.$$

**Remark 4.1.** *The non oscillating first-order corrector  $\tilde{T}_1$ , introduced in (19), is determined by the compatibility condition of the equation for  $T_3(x, y)$  in the unit cell: this is a standard computation (see [2], [6], [7], [14] for simpler models). It can also be obtained by taking a test function  $\phi_0 \neq 0$  in (43), at the end of the proof of Proposition 3.1 (see Remark 3.6). More precisely, we obtain*

$$\begin{aligned} -\operatorname{div}(K^*(x) \nabla \tilde{T}_1(x)) &= \sum_{i,j,k=1}^2 c_{ijk} \frac{\partial^3 T_0(x)}{\partial x_i \partial x_j \partial x_k} \\ &+ \sum_{i=1}^2 \left( m_i \frac{\partial T_0(x)}{\partial x_i} + d_i \frac{\partial F(x)}{\partial x_i} + g_i \frac{\partial H(x)(T_0(x) - T_{gas}(x))}{\partial x_i} \right) \end{aligned} \quad (49)$$

with

$$c_{ijk} = \int_{Y^S} \left[ \sum_{l=1}^2 K_{kl}(y) \frac{\partial \theta_{ij}}{\partial y_l}(y) - K_{ij}(y) \omega_k(y) \right] dy - \int_{\Gamma} G(y_k) (\theta_{i,j} + \omega_i y_j) dy,$$

$$m_i = \int_{\Gamma} h(y) \omega_i(y) dy,$$

$$d_i = \int_{Y^S} \sum_{j=1}^2 K_{ij}(y) \frac{\partial T_2^F}{\partial y_j}(y) dy - \int_{\Gamma} G(y_i) T_2^F dy,$$

$$g_i = \int_{Y^S} \sum_{j=1}^2 K_{ij}(y) \frac{\partial T_2^H}{\partial y_j}(y) dy - \int_{\Gamma} G(y_i) T_2^H dy.$$

The function  $\tilde{T}_1$  is not yet uniquely defined since we do not have any boundary condition for equation (49). It is customary to impose the same boundary conditions for  $\tilde{T}_1$  as for the homogenized solution  $T_0$ . However, we clearly see from the definition (48) of the boundary layer problem that changing the boundary condition for  $\tilde{T}_1$  is equivalent to changing the boundary condition for  $T_i^{bl,\epsilon}$ .

For the numerical computations concerning our industrial application, we shall simply ignore  $\tilde{T}_1$  and  $T_i^{bl,\epsilon}$ , namely take them equal to 0. On the other hand we choose  $T_1(x, y)$  being of zero average with respect to  $y$ . Note that,  $\tilde{T}_1 \equiv 0$  is a consequence of cubic symmetry assumptions for the coefficients in the periodicity cell  $Y$  (which imply that all parameters  $c_{i,jk}$ ,  $m_i$ ,  $g_i$  and  $d_i$  vanish). We do not have cubic symmetry of our reference cell (see Figure 2) but our numerical computations indicated that all values of these parameter are almost zero.

Based on the study of the first order boundary layer it was proved [7] for a pure conduction problem that one can get explicit convergence errors for the first order approximation of  $T_\epsilon$ . It is thus reasonable to conjecture that the same holds true in our context.

**Conjecture 4.1.** *The first order approximation of the solution  $T_\epsilon$  of (8) satisfies*

$$\|T_\epsilon - (T_0 + \epsilon T_1)\|_{L^2(\Omega_\epsilon)} \leq C\epsilon, \quad \|T_\epsilon - (T_0 + \epsilon T_1)\|_{H^1(\Omega_\epsilon)} \leq C\sqrt{\epsilon},$$

where the constant  $C$  does not depend on  $\epsilon$ .

Note that, because of boundary layers, the convergence speed in Conjecture 4.1 is not  $\epsilon^2$  and  $\epsilon$ , respectively, as could be expected from the (wrong) ansatz (14). On the same token, the convergence speed in Conjecture 4.1 is independent of the choice of the additive function  $\tilde{T}_1(x)$  in (19).

**Remark 4.2.** *Conjecture 4.1 is most probably valid for any geometry of the domain  $\Omega$  which may yield non trivial boundary layers. For the specific rectangular geometry under study, we are going to obtain in Section 6 a much better numerical convergence, typically*

$$\|T_\epsilon - (T_0 + \epsilon T_1)\|_{L^2(\Omega_\epsilon)} = \mathcal{O}(\epsilon^2),$$

*which means that the boundary layer  $T_1^{bl,\epsilon}$  is negligible. Because of this actual fact, it makes sense to look at the next term in the ansatz and to consider the second order corrector.*

As we shall see in Section 6, introducing  $T_2$  improves the qualitative behavior of the approximation but does not change the speed of convergence which is still

$$\|T_\epsilon - (T_0 + \epsilon T_1 + \epsilon^2 T_2)\|_{L^2(\Omega_\epsilon)} = \mathcal{O}(\epsilon^2).$$

In any case, it is clear that any mathematical justification of  $T_2$ , based on an error estimate similar to that in Conjecture 4.1, must rely on a preliminary asymptotic analysis of the non-oscillating first order corrector  $\tilde{T}_1$  and of the first order boundary layer  $T_1^{bl,\epsilon}(x)$ , a formidable task in which we do not want to endeavour. Therefore, we will merely numerically check that adding the second order corrector decreases significantly the error but not that the convergence speed is improved.

## 5 Non-linear case

As already discussed in Remark 2.2, the true physical problem involves a non-linear radiation operator, defined by formula (13) instead of (4). The study of the linear case was a simplifying assumption. However, the formal method of two-scale asymptotic expansion is perfectly valid in the non-linear case too (see [3]). In this section we give, without proof, the homogenization result in the non-linear case when Stefan-Boltzmann law applies, namely the emitted radiations are proportional to the 4th power of the temperature. More precisely, instead of using the linear formula (4) for  $G_\epsilon$  we use rather (13) with the emissivity  $e = 1$ , i.e.,

$$G_\epsilon(T_\epsilon)(s) = T_\epsilon^4(s) - \int_{\Gamma_{\epsilon,i}} T_\epsilon^4(x) F(s, x) dx \quad \forall s \in \Gamma_{\epsilon,i}.$$

The non-linear equivalent of Proposition 3.1 is the following.

**Proposition 5.1.** *Under assumption (14), the zero-order term  $T_0$  of the expansion for the solution  $T_\epsilon$  of (8) is the solution of the nonlinear homogenized problem*

$$\begin{cases} -\operatorname{div}\left(K^*(T_0^3)\nabla T_0(x)\right) + h^*(x)(T_0(x) - T_{gas}(x)) &= f^*(x) & \text{in } \Omega, \\ T_0(x) &= 0 & \text{on } \partial\Omega, \end{cases} \quad (50)$$

with the homogenized source  $f^*$  and exchange coefficient  $h^*$  given by (16). The homogenized conductivity tensor  $K^*$  depends on  $(T_0)^3$  and is given by its entries, for  $j, k = 1, 2$ ,

$$K_{j,k}^* = \frac{1}{|Y|} \left[ \int_{Y^S} K(e_j + \nabla_y \omega_j) \cdot (e_k + \nabla_y \omega_k) dy + 4\sigma T_0^3 \int_{\Gamma} G(\omega_k + y_k)(\omega_j + y_j) dy \right],$$

where  $G$  is the linear radiative operator defined by (12) and  $(\omega_k(x, y))_{1 \leq k \leq 2}$  are the solutions of the (linear) cell problems

$$\begin{cases} -\operatorname{div}_y \left( K(x, y)(e_j + \nabla_y \omega_j) \right) &= 0 & \text{in } Y^S, \\ K(x, y)(e_j + \nabla_y \omega_j) \cdot n &= 4\sigma T_0(x)^3 G(\omega_j + y_j) & \text{on } \Gamma, \\ y &\mapsto \omega_j(x, y) & \text{is } Y\text{-periodic.} \end{cases} \quad (51)$$

Furthermore, the first order corrector  $T_1(x, y)$  is still given by (19) and the second order corrector  $T_2(x, y)$  is the solution of

$$\begin{cases} -\operatorname{div}_y \left( K(x, y) [\nabla_y T_2(x, y) + \nabla_x T_1(x, y)] \right) = f(x, y) \\ \quad + \operatorname{div}_x \left( K(x, y) [\nabla_x T_0(x) + \nabla_y T_1(x, y)] \right) & \text{in } Y^S, \\ -K(x, y) [\nabla_y T_2(x, y) + \nabla_x T_1(x, y)] \cdot n = h(x, y) \left( T_0(x) - T_{gas}(x) \right) \\ \quad + 4\sigma T_0(x)^3 G \left( T_2 + \nabla_x T_1 \cdot y + \frac{1}{2} \nabla_x \nabla_x T_0 y \cdot y \right) \\ \quad - 4\sigma T_0(x)^3 G \left( \nabla_x T_1 + \nabla_x \nabla_x T_0 y \right) \cdot y & \text{on } \Gamma, \\ y \mapsto T_2(x, y) & \text{is } Y\text{-periodic.} \end{cases}$$

Corollary 3.1 becomes, in the non-linear case :

**Corollary 5.1.** *If we assume that the functions  $f$  and  $h$  satisfy (23) and that the conductivity tensor depends only on the microscopic variable, i.e.,  $K(x, y) \equiv K(y)$ , then, defining  $F^*$  and  $H^*$  by (24),  $T_2(x, y)$  can be written*

$$\begin{aligned} T_2(x, y) &= T_2^F(x, y)F(x) + T_2^H(x, y)H(x)(T_0(x) - T_{gas}(x)) \\ &\quad + \sum_{i,j=1}^2 \frac{\partial^2 T_0}{\partial x_i \partial x_j}(x) \theta_{i,j}(x, y) + \tilde{T}_2(x), \end{aligned}$$

where  $T_2^F$ ,  $T_2^H$  and  $\theta_{i,j}$  depend on  $x$  only through the value of  $T_0(x)^3$  and are solutions of the cell problems

$$\begin{cases} -\operatorname{div}_y (K(y) \nabla_y T_2^F(y)) &= f_{\#}(y) & \text{in } Y^S, \\ -K(y) \nabla_y T_2^F(y) \cdot n &= \frac{|Y|}{|\Gamma|} F^* + 4\sigma T_0(x)^3 G(T_2^F(y)) & \text{on } \Gamma, \\ T_2^F(y) &\text{is } Y\text{-periodic,} \end{cases} \quad (52)$$

$$\left\{ \begin{array}{ll} -\operatorname{div}_y(K(y)\nabla_y T_2^H(y)) &= 0 \quad \text{in } Y^S, \\ -K(y)\nabla_y T_2^H(y) \cdot n &= (h(y) - \frac{|Y|}{|\Gamma|} H^*) + 4\sigma T_0(x)^3 G(T_2^H(y)) \quad \text{on } \Gamma, \\ T_2^H(y) &\text{is } Y\text{-periodic,} \end{array} \right. \quad (53)$$

and

$$\left\{ \begin{array}{ll} -\operatorname{div}_y(K(y)[\nabla_y \theta_{i,j}(y) + e_j \omega_i(y)]) &= K_{i,j}(y) + K(y)\nabla_y \omega_i(y) \cdot e_j \quad \text{in } Y^S, \\ -K(y)[\nabla_y \theta_{i,j}(y) + e_j \omega_i(y)] \cdot n &= \frac{|Y|}{|\Gamma|} K_{i,j}^* \\ + 4\sigma T_0(x)^3 G\left(\theta_{i,j}(y) + \omega_i(y)y_j + \frac{1}{2}y_i y_j\right) - 4\sigma T_0(x)^3 G\left(\omega_i(y) + y_i\right)y_j &\quad \text{on } \Gamma, \\ \theta_{i,j}(y) &\text{is } Y\text{-periodic.} \end{array} \right. \quad (54)$$

Concerning the cell problems (of first or second order) the only difference with the linear case is that the constant  $\sigma$ , appearing in front of the linear radiative operator  $G$ , is replaced by  $4\sigma T_0(x)^3$  which arises from the linearization of the nonlinear operator. Concerning the homogenized problem (50), the only nonlinearity appears in the homogenized diffusion tensor  $K^*$  which depends on  $T_0^3$ .

## 6 Numerical results

In this section we describe some numerical experiments to study the asymptotic behaviour of the heat transfer model (8) in the non-linear case, i.e., when the radiation operator is defined as in Remark 2.2. Our goal is to show the efficiency of the proposed homogenization procedure, to validate it by comparing the reconstructed solution of the homogenized model with the numerical solution of the exact model (8) for smaller and smaller values of  $\epsilon$  and to exhibit a numerical rate of convergence in terms of  $\epsilon$ . Our computations do not take into account boundary layers nor the non oscillating part of the first-order corrector. All computations have been done with the finite element code CAST3M [12] developed at the French Atomic and Alternative Energy Commission (CEA).

### 6.1 Changing variables for the numerical simulation

Usually, in homogenization theory, a problem is homogenized in a fixed domain  $\Omega$  with cells of size  $\epsilon$  which tends to 0. However, in many practical applications (including ours for nuclear reactor physics), the size of the period is fixed (for physical reasons or manufacturing constraints) and it is rather the total number of cells, or equivalently the size of the domain, which is increasing. Therefore, following [3] and [4], we proceed differently: we fix the size of the periodicity cell (independent of  $\epsilon$ ) and we increase the total number of cells, i.e., the size of the global domain  $\widehat{\Omega} = \epsilon^{-1}\Omega = \prod_{j=1}^2(0, L_j/\epsilon)$  which is of order  $\epsilon^{-1}$ . In other words, instead of using the macroscopic space variable  $x \in \Omega$ , we use the microscopic

space variable  $y = x/\epsilon \in \widehat{\Omega}$ . For any function  $u(x)$  defined on  $\Omega$ , we introduce the rescaled function  $\widehat{u}(y)$ , defined on  $\widehat{\Omega}$  by

$$\widehat{u}(y) = u(\epsilon y) = u(x), \quad (55)$$

which satisfies  $\nabla_y \widehat{u}(y) = \epsilon(\nabla_x u)(\epsilon y) = \epsilon \nabla_x u(x)$ . All quantities defined in  $\widehat{\Omega}$  are denoted with a hat  $\widehat{\cdot}$  and, for simplicity, we drop the dependence on  $\epsilon$ . In this new frame of reference, the problem (8) becomes

$$\begin{cases} -\operatorname{div}(\widehat{K} \nabla \widehat{T}_\epsilon) &= \epsilon^2 \widehat{f}_\epsilon & \text{in } \widehat{\Omega}^S, \\ -\widehat{K} \nabla \widehat{T}_\epsilon \cdot n_S &= \epsilon^2 \widehat{h} \left( \widehat{T}_\epsilon - \widehat{T}_{gas} \right) + \sigma G_\epsilon(\widehat{T}_\epsilon) & \text{on } \widehat{\Gamma}, \\ \widehat{T}_\epsilon &= 0 & \text{on } \partial \widehat{\Omega}, \end{cases} \quad (56)$$

where  $\widehat{\Omega}^S$ ,  $\widehat{\Gamma}$  and  $\partial \widehat{\Omega}$  are defined by the same change of variables relating  $\Omega$  and  $\widehat{\Omega}$ . The homogenized problem (50) becomes

$$\begin{cases} -\operatorname{div}(\widehat{K}^*(\widehat{T}_0^3) \nabla \widehat{T}_0) + \epsilon^2 \widehat{h}^* \left( \widehat{T}_0 - \widehat{T}_{gas} \right) &= \epsilon^2 \widehat{f}^* & \text{in } \widehat{\Omega}, \\ \widehat{T}_0 &= 0 & \text{on } \partial \widehat{\Omega}. \end{cases} \quad (57)$$

The first order corrector  $\widehat{T}_1(y)$  is

$$\widehat{T}_1(y) = \epsilon T_1(\epsilon y, y) = \sum_{i=1}^2 \frac{\partial \widehat{T}_0}{\partial y_i}(y) \omega_i(y) + \widehat{\widetilde{T}}_1(y), \quad (58)$$

and the second order corrector  $\widehat{T}_2(y)$  is

$$\begin{aligned} \widehat{T}_2(y) &= \epsilon^2 T_2(\epsilon y, y) \\ &= \epsilon^2 T_2^F(y) \widehat{F}(y) + \epsilon^2 T_2^H(y) \widehat{H}(y) \left( \widehat{T}_0(y) - \widehat{T}_{gas}(y) \right) \\ &\quad + \sum_{i,j} \frac{\partial^2 \widehat{T}_0}{\partial y_i \partial y_j}(y) \theta_{i,j}(y) + \widehat{\widetilde{T}}_2(y). \end{aligned} \quad (59)$$

Finally, the homogenization approximation  $T_\epsilon(x) \simeq T_0(x) + \epsilon T_1(x, x/\epsilon) + \epsilon^2 T_2(x, x/\epsilon)$  becomes

$$\widehat{T}_\epsilon(y) \simeq \widehat{T}_0(y) + \widehat{T}_1(y) + \widehat{T}_2(y). \quad (60)$$

## 6.2 Algorithm and computational parameters

Our proposed algorithm for the homogenization process is the following.

1. Solve the 2 first order cell problems (51) for a range of values of  $\widehat{T}_0$ . Uniqueness of the solution  $\omega_i$  is insured by requiring that  $\int_Y \omega_i(x, y) dy = 0$ .



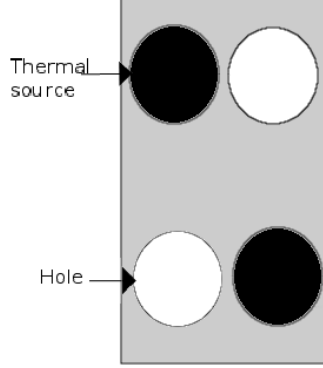


Figure 3: Support of the thermal source (black) in the reference cell  $Y^S$  (gray) perforated by holes (white).

2. Compute the homogenized conductivity (as a function of temperature) and the homogenized thermal source and heat exchange coefficient.
3. Solve the homogenized problem (50) by a fixed point algorithm.
4. Compute the first order corrector  $\widehat{T}_1(y) = \sum_{i=1}^2 \frac{\partial \widehat{T}_0}{\partial y_i}(y) \omega_i(\widehat{T}_0^3, y)$ .
5. Solve the 6 second order cell problems (52), (53), (54) for the homogenized temperature  $\widehat{T}_0$ .
6. Compute the second order corrector

$$\widehat{T}_2(y) = \epsilon^2 T_2^F(y) \widehat{F}(y) + \epsilon^2 T_2^H(y) \widehat{H}(y) (\widehat{T}_0(y) - \widehat{T}_{gas}(y)) + \sum_{i,j=1}^2 \frac{\partial^2 \widehat{T}_0}{\partial y_i \partial y_j}(y) \theta_{i,j}(y).$$

Although we did not write it explicitly, all correctors depend on  $\widehat{T}_0^3$ .

7. Reconstruct an approximate solution:  $\widehat{T}_0(y) + \widehat{T}_1(y) + \widehat{T}_2(y)$ .

We now give our computational parameters for a reference computation corresponding to  $\epsilon = \epsilon_0 = \frac{1}{4}$ . The geometry corresponds to a cross-section of a typical fuel assembly for a gas-cooled nuclear reactor (see [22] for further references). The domain is  $\widehat{\Omega} = \epsilon^{-1}\Omega = \prod_{j=1}^2 (0, L_j/\epsilon)$ , with, for  $j = 1, 2$ ,  $L_j/\epsilon = N_j \ell_j$  where  $N_1 = 3$ ,  $N_2 = 4$  and  $\ell_1 = 0.04m$ ,  $\ell_2 = 0.07m$ . Each periodicity cell contains 2 holes (see Figure 2), the radius of which is equal to  $0.0035m$ . Note that the unit cell is not a square but a rectangle of aspect ratio  $4/7$ . The emissivity of the holes boundaries is equal to  $e = 1$ . We enforce periodic boundary conditions in the  $x_1$  direction and Dirichlet boundary conditions in the other

direction which are given by  $\widehat{T}_\epsilon(y) = 800K$  on  $y_2 = 0m$  and  $\widehat{T}_\epsilon(y) = 1200K$  on  $y_2 = L_2/\epsilon = 0.28m$ . Although the reference cell is heterogeneous in the sense that it is made of at least two materials (graphite and the nuclear fuel), for simplicity we assume that the conductivity tensor  $K$  is constant and isotropic: its value is  $30Wm^{-1}K^{-1}$ . Similarly, the thermal exchange coefficient  $h$  is also constant throughout the domain. The physical value of the thermal exchange coefficient is  $\epsilon_0^2 \widehat{h} = 500 W.m^{-2}.K^{-1}$ , which takes into account the rescaling process adopted in Subsection 6.1. Hence  $\widehat{h} = 8000 W.m^{-2}.K^{-1}$ .

The oscillating thermal source is given by  $f_\#(y) = 7MW/m^3$  in disks strictly included in  $Y^S$  (with the same size as the holes) such that we have a source between each two fluid holes (in a checkerboard pattern, see Figure 3). The source is set to zero elsewhere. There is no macroscopic variation of the thermal source. In other words, from definition (23) we assume  $F(x) = 1$  in  $\Omega$ . The physical value of the thermal source is  $\epsilon_0^2 \widehat{f}_\# = 7MW/m^3$ . Hence  $\widehat{f}_\# = 112MW/m^3$ .

Remark that it is only for the reference computation  $\epsilon_0 = 1/4$  that  $\widehat{f}_\#$  and  $\widehat{h}$  are equal to their physical values. While the rescaled coefficients  $\widehat{f}_\#$  and  $\widehat{h}$  are varying with  $\epsilon$ , the original coefficients  $f_\#$  and  $h$  are independent of  $\epsilon$ . The fact that the numerical values of  $\epsilon^2 \widehat{f}_\#$  and  $\epsilon^2 \widehat{h}$  are not the physical ones for  $\epsilon \neq \epsilon_0 = 1/4$  is not a problem, since our convergence study (as  $\epsilon$  goes to 0) is purely a numerical verification of our mathematical result.

All computations are performed with rectangular  $\mathbb{Q}_1$  finite elements (4 nodes in 2D). A boundary integral method is used for the radiative term (which involves a dense matrix coupling all nodes on the surface enclosing the holes). The typical number of nodes for the 2D cell problem is 1 061 (from which 72 are on the radiative boundary  $\gamma$ ); it is 656 for the homogenized problem (which has no radiative term); it is 12 249 for the original problem (8) with  $\epsilon = \epsilon_0 = \frac{1}{4}$  (from which 864 are on the radiative boundary  $\Gamma_\epsilon$ ).

**Remark 6.1.** *Since the thermal exchange coefficient  $h$  is constant the second-order corrector  $T_2^H$  vanishes. The other second-order corrector  $\frac{\partial^2 \widehat{T}_0}{\partial y_i \partial y_j}(y) \theta_{i,j}(y)$  is small since the homogenized solution  $\widehat{T}_0$  is slowly varying and its second-order derivatives is of order  $\epsilon^2$ . The only term which is not negligible is  $\epsilon^2 T_2^F(y) \widehat{F}(y)$  if the source term is large (this is the only corrector term depending on the source term as already said in Remark 3.4). The importance of  $\epsilon^2 T_2^F(y) \widehat{F}(y)$  can be checked on Figures 15, 16 and 17 which are plotted for three different orders of magnitude of the source term.*

### 6.3 Simulation results

We start this section by comparing, in the reference configuration  $\epsilon = \epsilon_0 = 1/4$ , the direct solution of the problem (8) in the non-linear case, with the solution of the homogenized problem (50) plus the correctors  $\widehat{T}_1$  and  $\widehat{T}_2$ . The homogenized problem parameters are

$$\widehat{f}^*(x) = \widehat{F}^* = \frac{1}{|Y|} \int_{Y^S} f_\#(y) dy = 17,8174 MW/m^3,$$

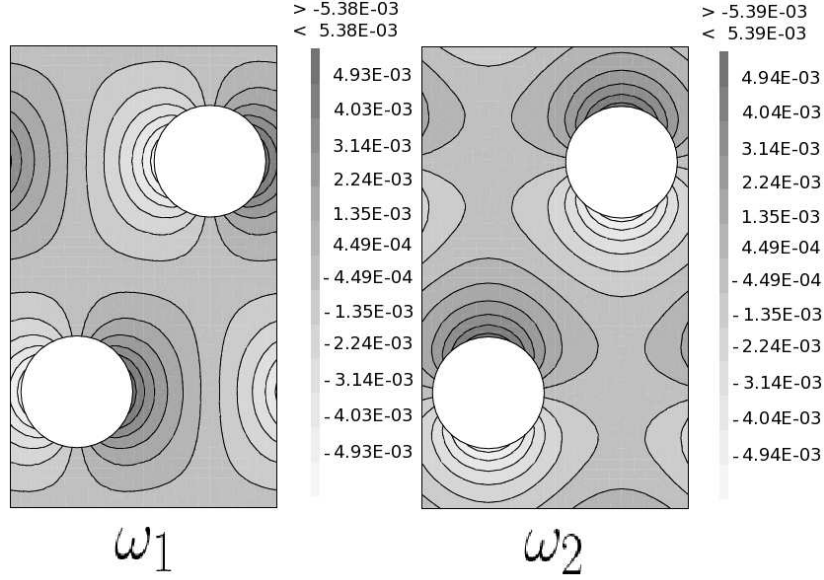


Figure 4: Solutions of the first order cell problems (51) for  $\widehat{T}_0 = 800K$ :  $\omega_1$  (left),  $\omega_2$  (right).

$$\widehat{h}^*(x) = \widehat{H}^* = \frac{|\Gamma|}{|Y|} \widehat{h} = 0,319383 \text{ MW.m}^{-2} \cdot K^{-1}.$$

To compute the homogenized conductivity, we compute the solutions of the cell problems (51) what we plot in Figure 4 for an homogenized temperature  $T_0 = 800K$ . Recall that, in the non linear case, the solutions of the cell problems depend on the macroscopic temperature. These solutions of (51) are uniquely determined because we choose them being of zero average in the cell.

The cell solutions allow us to evaluate the homogenized conductivity which turns out to numerically be a diagonal tensor (at least for temperatures  $T_0 \leq 1E + 05K$  with a precision on 14 digits). However, for larger (extreme) temperatures,  $\widehat{K}^*$  is not any longer a diagonal tensor [3] since the unit cell is not a square but a rectangle of aspect ratio 4/7. The diagonal entries of  $\widehat{K}^*$  are plotted on Figure 5 and two typical values are

$$\widehat{K}^*(\widehat{T}_0 = 50K) = \begin{pmatrix} 25.907 & 0. \\ 0. & 25.914 \end{pmatrix}, \quad \widehat{K}^*(\widehat{T}_0 = 20000K) = \begin{pmatrix} 49.801 & 0. \\ 0. & 49.781 \end{pmatrix}.$$

By a fixed point algorithm (the homogenized conductivity  $\widehat{K}^*$  is evaluated with the previous iterate for the temperature), we solve the homogenized problem (it requires of the order of 5 iterates). By a Newton method we solve also the direct model (56) (it requires of the order of 15 iterates). The solutions of the second order cell problems (52) and (54) are displayed on Figures 6 and 7. We choose the unknown additive constant for these solutions in such a way

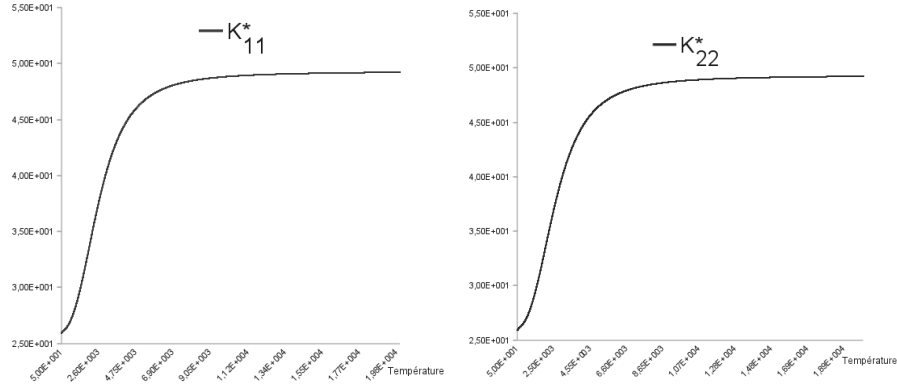


Figure 5: Homogenized conductivity as a function of the macroscopic temperature  $T_0$ :  $\widehat{K}^*_{11}$ (left),  $\widehat{K}^*_{22}$ (right).

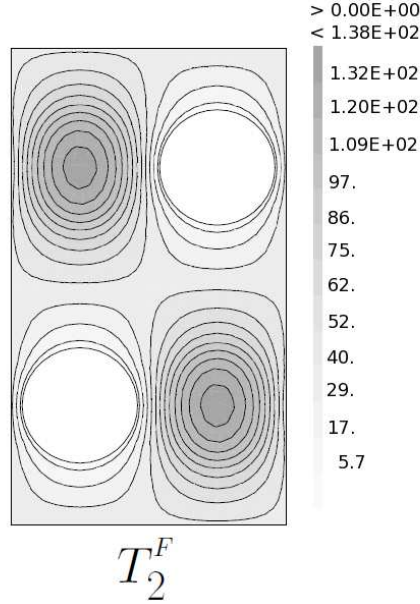


Figure 6: Solution  $T_2^F$  of the second order cell problem (52).

that they are almost equal to zero on the holes' boundaries. Since the exchange coefficient  $h$  is constant, the other second order cell problem (53) does not need to be solved: its solution is always zero.

In Figure 8 we plot the direct, homogenized and reconstructed solutions computed for a value of  $\epsilon = \epsilon_0 = 1/4$ . The reconstructed solution  $\widehat{T}_0 + \widehat{T}_1$  is a better approximation of the true solution  $\widehat{T}_\epsilon$  than the mere homogenized

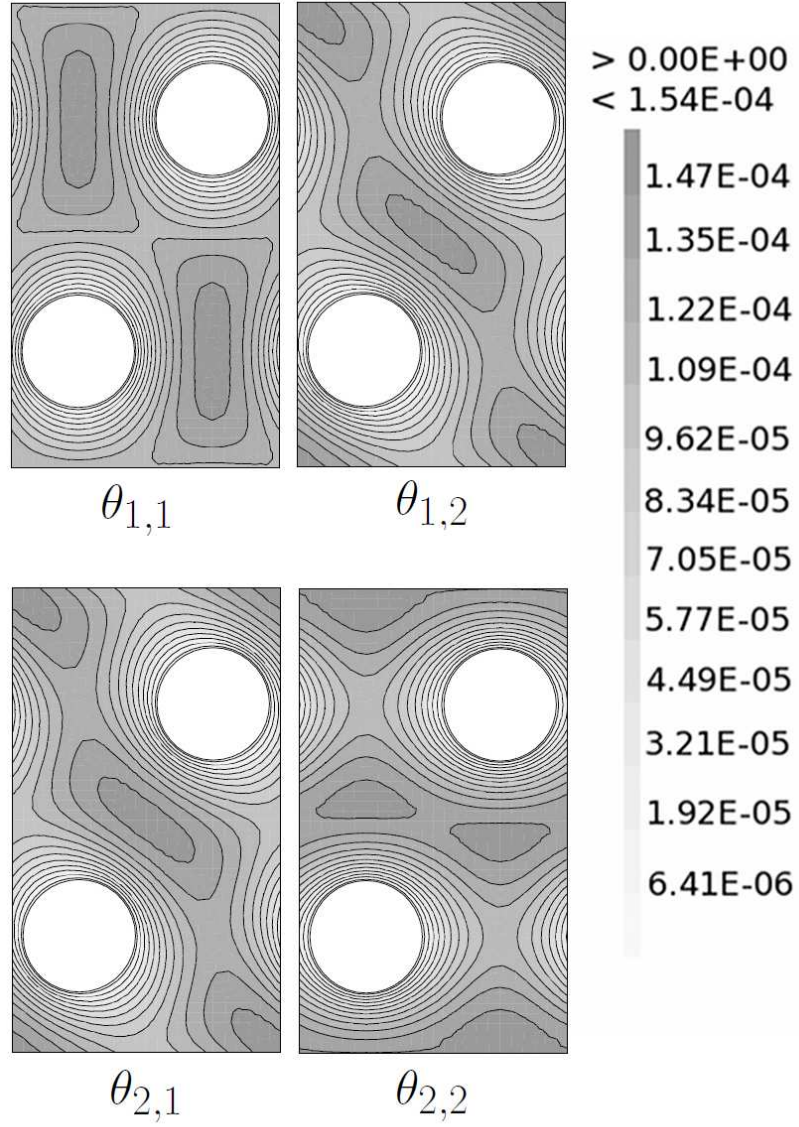


Figure 7: Solutions  $\theta_{i,j}$ ,  $i, j = 1, 2$ , of the second order cell problem (54).

solution  $\hat{T}_0$ . Clearly the reconstructed solution  $\hat{T}_0 + \hat{T}_1 + \hat{T}_2$  is a much better approximation than  $\hat{T}_0 + \hat{T}_1$ , especially in the region between holes where large temperature gradients occur from the source supports to the holes. Even more convincingly, we display the modules of the temperature gradients in Figure 9

and the modules of the gradient error approximations in Figure 10.

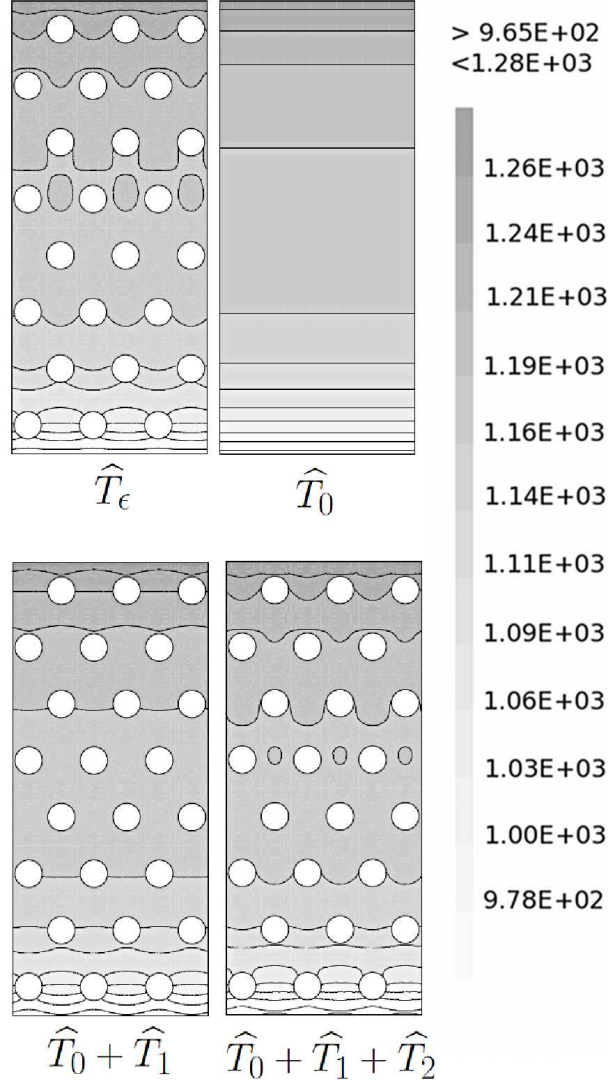


Figure 8: Direct solution  $\hat{T}_\epsilon$  (top left), homogenized solution  $\hat{T}_0$  (top right),  $\hat{T}_0 + \hat{T}_1$  (bottom left) and  $\hat{T}_0 + \hat{T}_1 + \hat{T}_2$  (bottom right).

**Remark 6.2.** To justify (at least numerically) our choice of neglecting  $\tilde{T}_1$  in the reconstruction process (60), following the notations of Remark 4.1, we compute

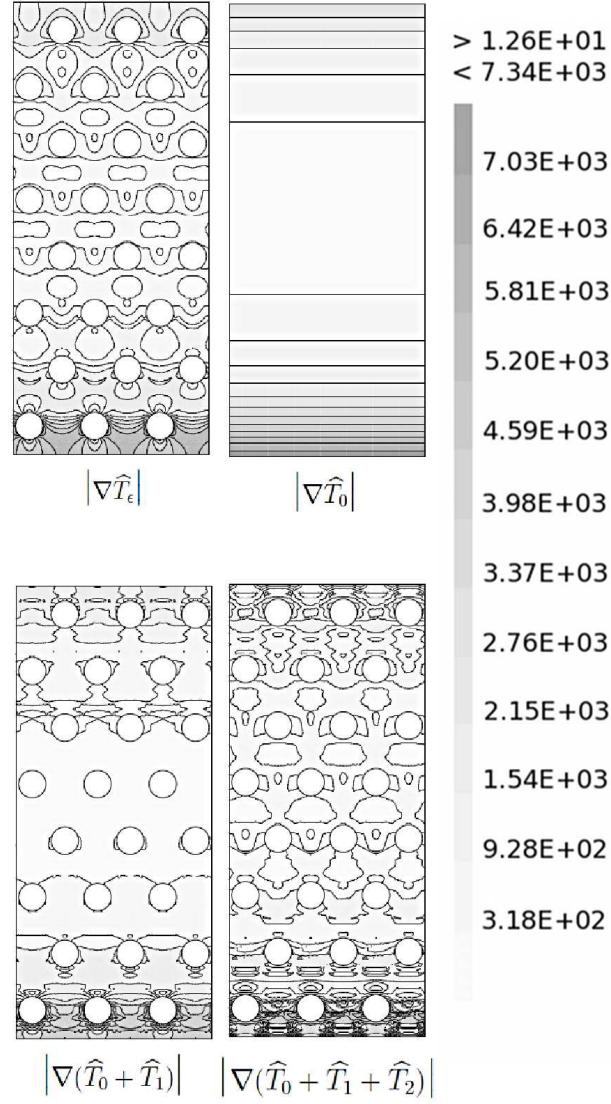


Figure 9: Modules of the solution gradients in  $\widehat{\Omega}$ :  $|\nabla \widehat{T}_\epsilon|$  (top left),  $|\nabla \widehat{T}_0|$  (top right),  $|\nabla(\widehat{T}_0 + \widehat{T}_1)|$  (bottom left) and  $|\nabla(\widehat{T}_0 + \widehat{T}_1 + \widehat{T}_2)|$  (bottom right).

the parameters  $c_{ijk}$ ,  $d_i$ ,  $m_i$  and  $g_i$  which appear in the equation for  $\widetilde{T}_1$ . Their values are equal to

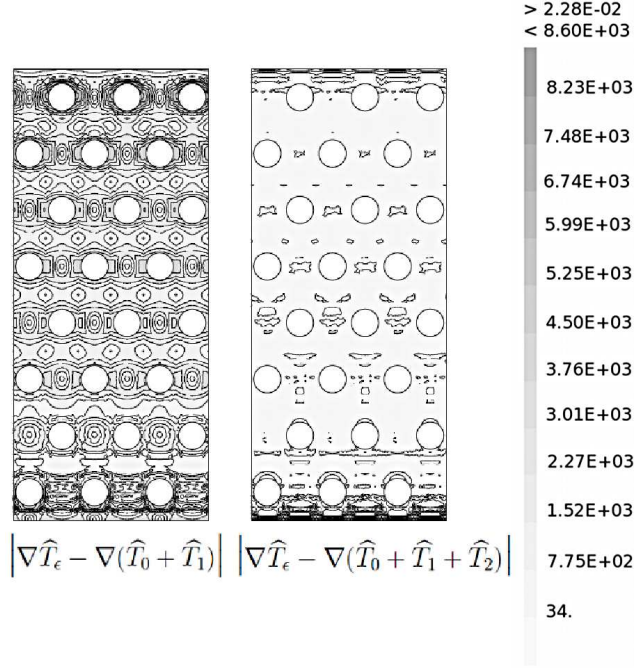


Figure 10: Modules of the solution gradients error in  $\widehat{\Omega}$ :  $|\nabla \widehat{T}_\epsilon - \nabla(\widehat{T}_0 + \widehat{T}_1)|$  (left) and  $|\nabla \widehat{T}_\epsilon - \nabla(\widehat{T}_0 + \widehat{T}_1 + \widehat{T}_2)|$  (right).

$c_{111}$	$=$	$-2.42128E-10$	$m_1$	$=$	$0.$
$c_{112}$	$=$	$3.37167E-10$	$m_2$	$=$	$0.$
$c_{121}$	$=$	$-3.11185E-21$			
$c_{122}$	$=$	$-1.49058E-21$	$d_1$	$=$	$0.$
$c_{211}$	$=$	$2.32272E-21$	$d_2$	$=$	$0.$
$c_{212}$	$=$	$-4.46678E-23$			
$c_{221}$	$=$	$-2.42128E-10$	$g_1$	$=$	$0.$
$c_{222}$	$=$	$3.37167E-10$	$g_2$	$=$	$0.$

Together with a homogeneous Dirichlet boundary condition, it implies that  $\tilde{T}_1$ , solution of (49), is approximately zero.

In order to better show the influence of the second order corrector  $T_2$  we plot the different solutions, exact  $\widehat{T}_\epsilon$ , homogenized  $\widehat{T}_0$ , first order approximation  $(\widehat{T}_0 + \widehat{T}_1)$  and second order approximation  $(\widehat{T}_0 + \widehat{T}_1 + \widehat{T}_2)$  on various line segments for  $\epsilon = 1/4$ . On Figure 11 we plot the profile segments:  $D_1 = (a_1; a_2)$  with  $a_1 = (L_1/2, 0)$  and  $a_2 = (L_1/2, L_2/\epsilon)$ ,  $D'_1 = (a'_1; a'_2)$  with  $a'_1 = a_1$  and  $a'_2 = (L_1/2, 3L_2/5\epsilon)$ ,  $D''_1 = (a''_1; a''_2)$  with  $a''_1 = (L_1/2, 7L/16\epsilon)$  and  $a''_2 = (L_1/2, 9L/16\epsilon)$ ,  $P_1 = (b_1; b_2)$  with  $b_1 = (1.75263E - 02, 2.0625E - 02/\epsilon)$



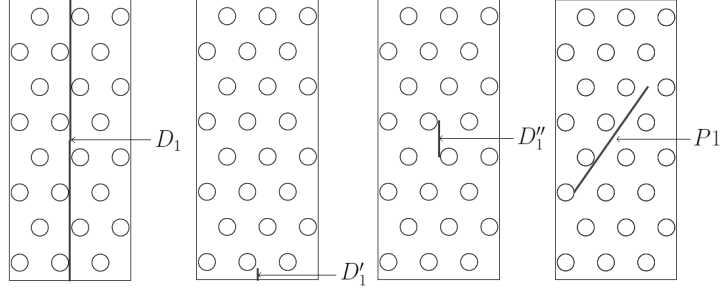


Figure 11: From left to right, the line segments  $D_1$ ,  $D_1'$ ,  $D_1''$  and  $P_1$  for  $\epsilon = 1/4$ .

and  $b_2 = (8.72628E - 02, 4.5375E - 02/\epsilon)$ . Along  $D_1$  (and its subsets  $D_1'$  and  $D_1''$ ) there is no source term: thus the influence of  $T_2$  is almost negligible (see Figure 12). Along  $P_1$  the source term is oscillating from 0 to its nominal value: the influence of  $T_2$  is dramatic (see Figure 15).

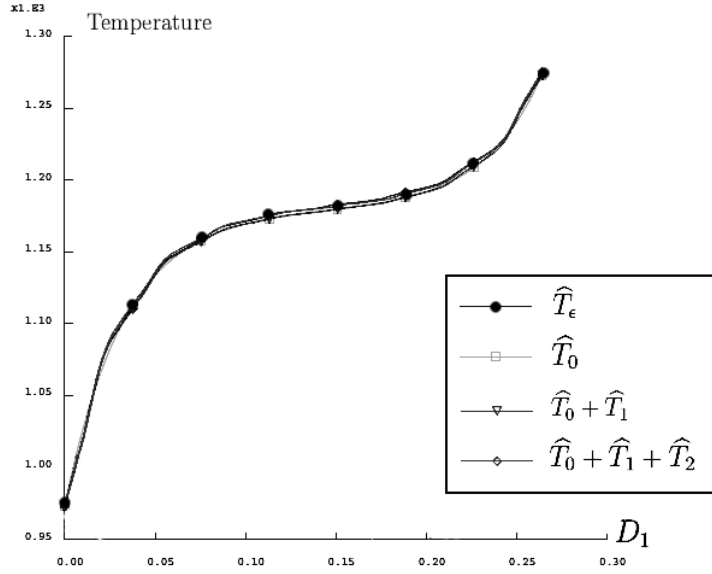


Figure 12: Different solutions along the line segment  $D_1$ .

Since there are not much variations between the different solutions in Figure 12, we display two different zooms in Figures 13 and 14. On the sub-segment  $D_1''$  (in the middle of the domain  $\hat{\Omega}$ ) the second order approximation is better than the first order one, as we could expect (see Figure 14). However, on the sub-segment  $D_1'$  (close to the boundary of  $\hat{\Omega}$ ) the second order corrector  $\hat{T}_2$  adds an additional error close the boundary  $y_2 = 0$  since it does not satisfy a homogeneous Dirichlet boundary condition (see Figure 13).

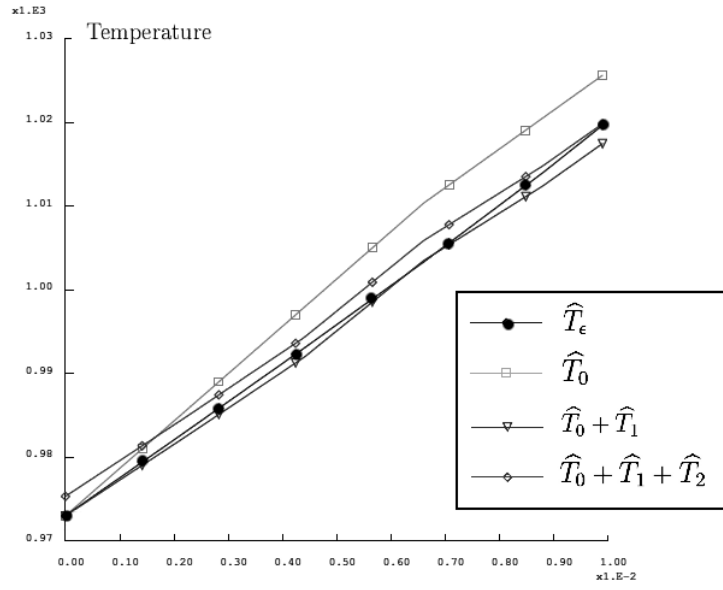


Figure 13: Different solutions along the line segment  $D'_1$ .

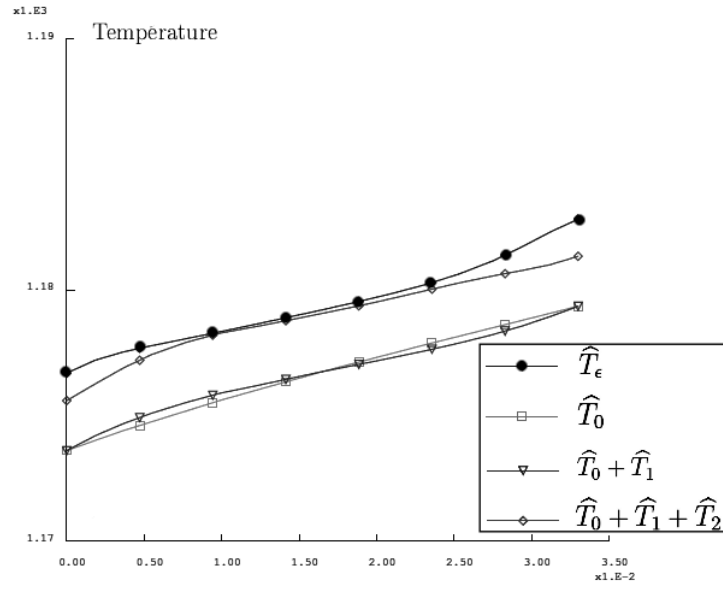


Figure 14: Different solutions along the line segment  $D''_1$ .

To check that the importance of the second order corrector is directly linked to the amplitude of the source term (as is obvious in view of the cell problem

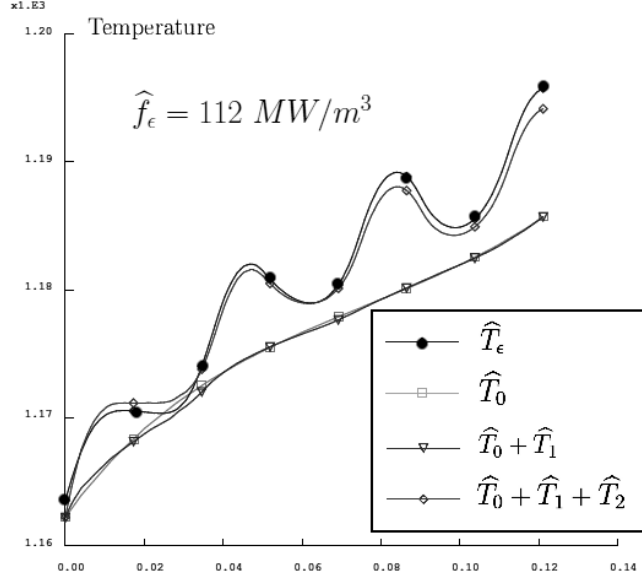


Figure 15: Different solutions along the line segment  $P_1$  for  $\hat{f}_\epsilon = 112 \text{ MW}/m^3$ .

(52) for  $T_2^F$ ), we re-do the same plot of Figure 15 with a different magnitude of the source term. Not surprisingly, when  $\hat{f}_\epsilon = 0 \text{ MW}/m^3$  there are almost no differences between the different approximations (see Figure 16), while for  $\hat{f}_\epsilon = 16000 \text{ MW}/m^3$ , the second order approximation is the only one to follow closely the true solution (see Figure 17). For more numerical results (different values of  $\epsilon$ , different values of  $\hat{h}_\epsilon$ , etc.), we refer the interested reader to [22].

Eventually, to check the convergence of the homogenization process and to obtain a numerical speed of convergence as the small parameter  $\epsilon$  goes to 0, we display in Figure 18 the relative errors (61) on the temperature, as functions of  $\epsilon$  on a log-log scale. In practice, the limit as  $\epsilon$  goes to 0 is obtained by increasing the number of cells and we obtain the following sequence of values:  $\epsilon = 1/4, 1/8, 1/12, 1/16, 1/20, 1/24, 1/28, 1/32, 1/36$ .

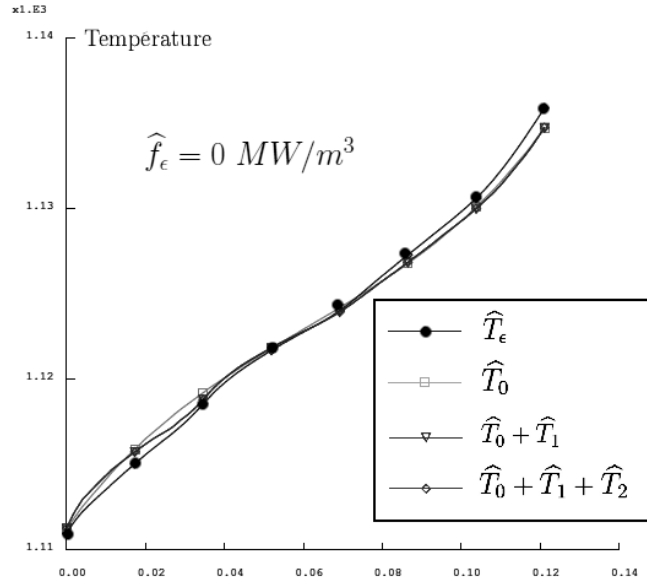


Figure 16: Different solutions along  $P_1$  for  $\hat{f}_\epsilon = 0 \text{ MW/m}^3$ .

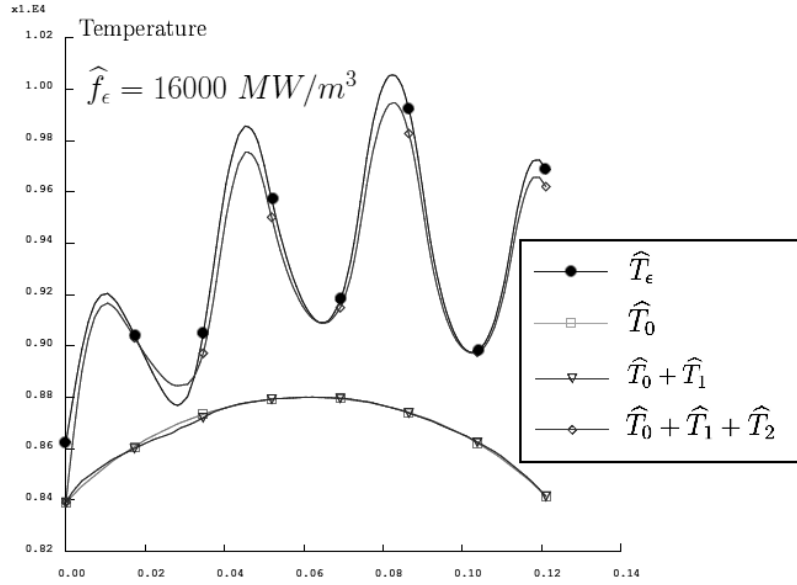


Figure 17: Different solutions along  $P_1$  for  $\hat{f}_\epsilon = 16000 \text{ MW/m}^3$ .

We compare the obtained errors (61) with the slopes of  $\epsilon$ ,  $\epsilon^2$  and  $\epsilon^3$ .

$$\left\{ \begin{array}{l} ERR(T)_0 = \frac{\|\hat{T}_\epsilon(y) - (\hat{T}_0(y))\|_{L^2(\hat{\Omega})}}{\|\hat{T}_\epsilon(y)\|_{L^2(\hat{\Omega})}}, \\ ERR(T)_1 = \frac{\|\hat{T}_\epsilon(y) - (\hat{T}_0(y) + \hat{T}_1(y))\|_{L^2(\hat{\Omega})}}{\|\hat{T}_\epsilon(y)\|_{L^2(\hat{\Omega})}}, \\ ERR(T)_2 = \frac{\|\hat{T}_\epsilon(y) - (\hat{T}_0(y) + \hat{T}_1(y) + \hat{T}_2(y))\|_{L^2(\hat{\Omega})}}{\|\hat{T}_\epsilon(y)\|_{L^2(\hat{\Omega})}}, \end{array} \right. \quad (61)$$

Once again we recall that our reconstructions  $(\widehat{T}_0 + \widehat{T}_1)$  and  $(\widehat{T}_0 + \widehat{T}_1 + \widehat{T}_2)$  do not feature any boundary layers nor non-oscillating corrector terms.

The error  $ERR(T)_0$  behaves like  $\epsilon$  as we can expect. Although, we could not prove rigorously anything about  $ERR(T)_1$  and  $ERR(T)_2$ , we check on Figure 18 that they both behave as  $\epsilon^2$ . This implicitly implies that the first order boundary layer is indeed negligible. Although  $ERR(T)_2$  has the same slope as  $ERR(T)_1$  on Figure 18, it is much smaller.

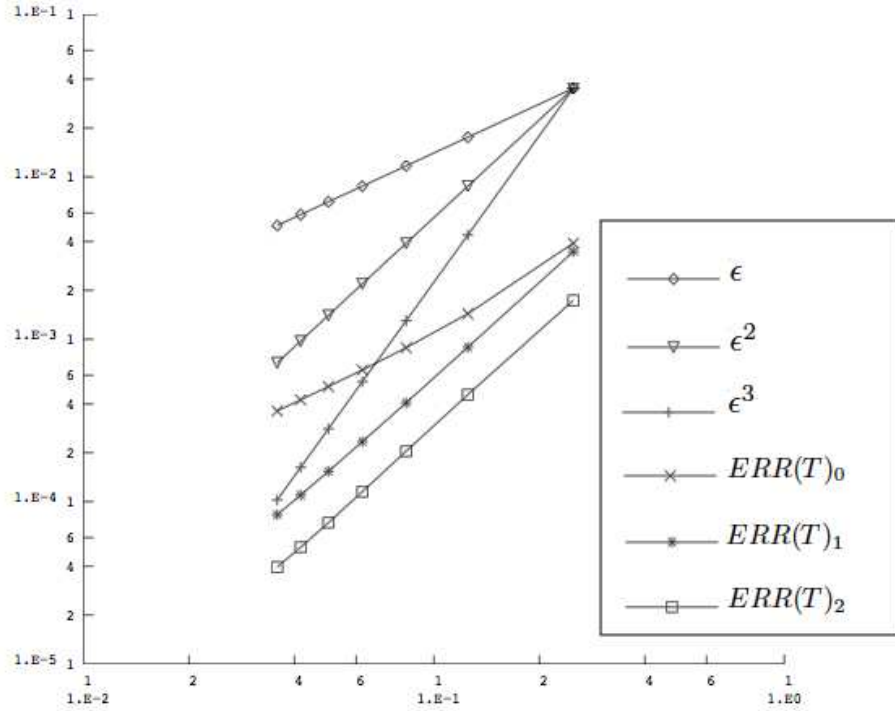


Figure 18: Relative temperature errors as a function of  $\epsilon$ .

As a conclusion of our numerical analysis, we claim that, even if the second order corrector  $T_2$  does not improve the convergence order of the homogenization process, for a fixed value of  $\epsilon$  it improves the qualitative behavior of the reconstructed solution and it decreases the relative error all the more when the source term is locally varying with a large amplitude. In industrial practice,  $\epsilon$  is never going to zero, so these two achievements are more than enough to justify the use of the second order corrector in the numerical homogenization of the heat transfer problem (8). Recall that computing a first-order, or even second-order, reconstructed homogenized solution is much cheaper than computing a direct solution of the original problem since the latter one requires a very fine mesh of size smaller than  $\epsilon$ .

## References

- [1] G. Allaire. Homogenization and two-scale convergence. *SIAM J. Math. Anal.*, 23(6):1482–1518, 1992.
- [2] G. Allaire and M. Amar. Boundary layer tails in periodic homogenization. *ESAIM Control Optim. Calc. Var.*, 4:209–243, 1999.
- [3] G. Allaire and K. El Ganaoui. Homogenization of a conductive and radiative heat transfer problem. *Multiscale Model. Simul.*, 7(3):1148–1170, 2008.
- [4] G. Allaire and Z. Habibi. Homogenization of a conductive, convective and radiative heat transfer problem. *submitted*. Internal report, n. 746, CMAP, Ecole Polytechnique (March 2012). <http://www.cmap.polytechnique.fr/preprint/repository/746.pdf>
- [5] A. A. Amosov. Stationary nonlinear nonlocal problem of radiative-conductive heat transfer in a system of opaque bodies with properties depending on radiation frequency. *J. Math. Sci.*, 164(3):309–344, 2010.
- [6] N. Bakhvalov and G. Panasenko. *Homogenisation: averaging processes in periodic media*, volume 36 of *Mathematics and its Applications (Soviet Series)*. Kluwer Academic Publishers Group, Dordrecht, 1989. Mathematical problems in the mechanics of composite materials, Translated from the Russian by D. Leites.
- [7] A. Bensoussan, J. L. Lions, and G. Papanicolaou. *Asymptotic analysis for periodic structures*, volume 5 of *Studies in Mathematics and its Applications*. North-Holland Publishing Co., Amsterdam, 1978.
- [8] J.-F. Bourgat, *Numerical experiments of the homogenization method for operators with periodic coefficients*, Computing methods in applied sciences and engineering (Proc. Third Internat. Sympos., Versailles, 1977), I, pp. 330–356, Lecture Notes in Math., 704, Springer, Berlin (1979).
- [9] J.-F. Bourgat, A. Dervieux, *Méthode d’homogénéisation des opérateurs à coefficients périodiques: étude des correcteurs provenant du développement asymptotique*, IRIA-LABORIA, Rapport n.278 (1978).
- [10] S. Boyaval. Reduced-bases approach for homogenization beyond the periodic setting. *Multiscale Model. Simul.*, 7(1):466–494, 2008.
- [11] J. Casado-Daz, The asymptotic behaviour near the boundary of periodic homogenization problems via two-scale convergence. *Proc. Roy. Soc. Edinburgh Sect. A*, 138 (2008), no. 1, 33–66.
- [12] Cast3M. <http://www-cast3m cea.fr/cast3m/index.jsp>.
- [13] S. Chandrasekhar. *Radiative transfer*. Dover Publications Inc., New York, 1960.

- [14] K. Cherednichenko, V. Smyshlyaev. *On full two-scale expansion of the solutions of nonlinear periodic rapidly oscillating problems and higher-order homogenised variational problems*. Arch. Ration. Mech. Anal. 174 (2004), no. 3, 385–442.
- [15] D. Cioranescu and P. Donato. *An introduction to homogenization*, volume 17 of *Oxford Lecture Series in Mathematics and its Applications*. The Clarendon Press Oxford University Press, New York, 1999.
- [16] CEA e-den. *Les réacteurs nucléaires à caloporteur gaz*. CEA Saclay et Le Moniteur Editions. Monographie Den, 2006. <http://nucleaire.cea.fr/fr/publications/pdf/M0-fr.pdf>.
- [17] C. Conca, R. Orive, M. Vanninathan, *First and second corrector in homogenization by Bloch waves*, (Spanish. Spanish summary) Bol. Soc. Esp. Mat. Apl. SēMA No. 43 (2008), 61–69.
- [18] D. Gérard-Varet, N. Masmoudi, *Homogenization in polygonal domains*, J. Eur. Math. Soc., 13, 1477–1503 (2011).
- [19] D. Gérard-Varet, N. Masmoudi, *Homogenization and boundary layer*, to appear in Acta Mathematica.
- [20] G. Griso, *Interior error estimate for periodic homogenization*, Anal. Appl. (Singap.) 4 (2006), no. 1, 61–79.
- [21] Z. Habibi. Homogenization of a conductive-radiative heat transfer problem, the contribution of a second order corrector. *ESAIM proc.* (submitted).
- [22] Z. Habibi. *Homogénéisation et convergence à deux échelles lors d'échanges thermiques stationnaires et transitoires dans un coeur de réacteur à caloporteur gaz*. PhD thesis, Ecole Polytechnique, 2011. <http://tel.archives-ouvertes.fr/tel-00695638>
- [23] P.S. Heckbert. *Simulating global illumination using Adaptive Meshing*. PhD thesis, UC Berkeley, 1991.
- [24] V.H. Hoang, Ch. Schwab, *High-dimensional finite elements for elliptic problems with multiple scales*, Multiscale Model. Simul. 3, no. 1, 168–194 (2004/05).
- [25] U. Hornung, editor. *Homogenization and porous media*, volume 6 of *Interdisciplinary Applied Mathematics*. Springer-Verlag, New York, 1997.
- [26] J. R. Howell. *A catalogue of radiation heat transfer factors*. The university of Texas at Austin, Austin, Texas, 3 edition, 2010. <http://www.engr.uky.edu/rtl/Catalog/>.
- [27] V. V. Jikov, S. M. Kozlov, and O. A. Oleinik. *Homogenization of Differential Operators and Integral Functionals*. Springer Verlag, 1994.

- [28] C. Kenig, F. Lin and Z. Shen, Convergence Rates in  $L^2$  for Elliptic Homogenization Problems, *Arch. Ration. Mech. Anal.* 203 (2012), no. 3, 1009–1036.
- [29] M. Laitinen and T. Tiihonen. Conductive-radiative heat transfer in grey materials. *Quart. Appl. Math.*, 59(4):737–768, 2001.
- [30] J. L. Lions. *Some methods in the mathematical analysis of systems and their control*. Kexue Chubanshe (Science Press), Beijing, 1981.
- [31] Y. Maday, A. T. Patera, and G. Turinici. Global a priori convergence theory for reduced-basis approximations of single-parameter symmetric coercive elliptic partial differential equations. *C. R. Math. Acad. Sci. Paris*, 335(3):289–294, 2002.
- [32] F. M. Modest. *Radiative heat transfer*. Academic Press, 2 edition, 2003.
- [33] S. Moskow and M. Vogelius, *First-order corrections to the homogenised eigenvalues of a periodic composite medium. A convergence proof*. Proc. Roy. Soc. Edinburgh Sect. A, 127, no. 6, 1263–1299 (1997).
- [34] G. Nguetseng. A general convergence result for a functional related to the theory of homogenization. *SIAM J. Math. Anal.*, 20(3):608–623, 1989.
- [35] D. Onofrei, B. Vernescu, Error estimates for periodic homogenization with non-smooth coefficients, *Asymptot. Anal.*, 54 (2007), no. 1-2, 103–123.
- [36] E. Sanchez-Palencia. *Nonhomogeneous media and vibration theory*, volume 127 of *Lecture Notes in Physics*. Springer-Verlag, Berlin, 1980.
- [37] L. Tartar. *The general theory of homogenization. A personalized introduction. Lecture Notes of the Unione Matematica Italiana*. Springer Verlag, Berlin; UMI, Bologna, 7 edition, 2009.
- [38] T. Tiihonen. Stefan-boltzman radiation on non-convex surfaces. *Math. Methods Appl. Sci.*, 20:47–57, 1997.
- [39] T. Tiihonen. Finite element approximation of nonlocal heat radiation problems. *Math. Models Methods Appl. Sci.*, 8(6):1071–1089, 1998.